

Heavy-tailed Distributions In Stochastic Dynamical Models

Ph. Blanchard^{1,2}, T. Krüger² D. Volchenkov² ¹

¹ *Department of Physics, Universität Bielefeld, Postfach 10 01 31, 33501 Bielefeld, Germany*

² *Center of Excellence Cognitive Interaction Technology, Universität Bielefeld, Postfach 10 01 31, 33501 Bielefeld, Germany*

¹E-Mail: volchenk@physik.uni-bielefeld.de

Heavy-tailed Distributions In Stochastic Dynamical Models

Ph. Blanchard^{1,2}, T. Krüger² D. Volchenkov² ¹

Abstract

Heavy-tailed distributions are found throughout many naturally occurring phenomena. We have reviewed the models of stochastic dynamics that lead to heavy-tailed distributions (and power law distributions, in particular) including the multiplicative noise models, the models subjected to the Degree-Mass-Action principle (the generalized preferential attachment principle), the intermittent behavior occurring in complex physical systems near a bifurcation point, queuing systems, and the models of Self-organized criticality. Heavy-tailed distributions appear in them as the emergent phenomena sensitive for coupling rules essential for the entire dynamics.

Keywords: Heavy-tailed distributions, Preferential attachment, Intermittency, Queueing systems, Self-organized criticality

Contents

1	Introduction	3
2	Degree-Mass-Action principle in random graphs formation	6
2.1	A random graph space of the preferential attachment model . . .	6
2.2	The Cameo Principle. The origins of scale-free graphs in social networks.	8
3	The statistics of bursts in systems close to a threshold of instability	11
3.1	Systems at a threshold of instability	12
3.2	Distribution of residence times below the threshold	13
3.2.1	Some examples of decay in the correlated case $\eta = 1$. . .	15
3.2.2	Upper and lower bounds for $P(T)$ for any η	16
3.2.3	Behavior of $P(T)$ for intermediate times	17
3.3	Distribution of quiescent times for the case of uniform densities .	17

¹E-Mail: volchenk@physik.uni-bielefeld.de

4	Fat tails in queuing systems	21
4.1	Waiting time distributions for queuing systems with fat tail service times	23
4.2	Scheduling based on time dependent priority indexes	24
4.2.1	Tasks population dynamics with time dependent priority indexes	24
4.2.2	Stochastic dynamics. Real-time queuing dynamics	27
4.2.3	"First come first served" (FCFS) scheduling policies	30
4.3	The importance of adopting performance scheduling policies	33
5	Power law distributions in Self-Organized Criticality	34
5.1	Coarse-graining of microscopic evolution rules for SOC-models	36
5.2	Covariance of random forces	39
5.3	An infinite number of critical regimes in SOC- models	42
5.4	Fat tails in SOC-models	43
6	Conclusions	45
7	Acknowledgments	46

1. Introduction

In 1906, a lecturer in economics at the University of Lausanne in Switzerland V.F. Pareto had discovered that the allocation of wealth among individuals can be efficiently described by a *power law* probability distribution, as being self-similar over a wide range of wealth magnitudes. A great many such distributions have been found in diverse fields of science being a long-known feature of many empirical distributions such as Pareto, Zipf, and Lévy distributions used to model real-world phenomena. In particular, Paul Lévy worked on a class of probability distributions with "heavy tails", which he called *stable distributions* largely considered probabilistic curiosities at the time, as heavy-tailed distributions have properties that are qualitatively different to the many commonly used distributions such as exponential, normal or Poisson.

Since then, there has been a permanent surge of interest to heavy-tailed and power law distributions from scientists working in fields as diverse as weather forecasting to stock market analysis. The growth rate of the interest to the heavy-tailed and power law distributions can be attested by the yearly increase of the total number of publications on the topic (see Fig. 1) in the arXiv (<http://arxiv.org>), the major forum for disseminating scientific results in Physics, Mathematics, Nonlinear Sciences, Computer Science, and Quantitative Biology.

The purpose of this review paper is to explain the models of stochastic dynamics that lead to heavy-tailed and power law distributions.

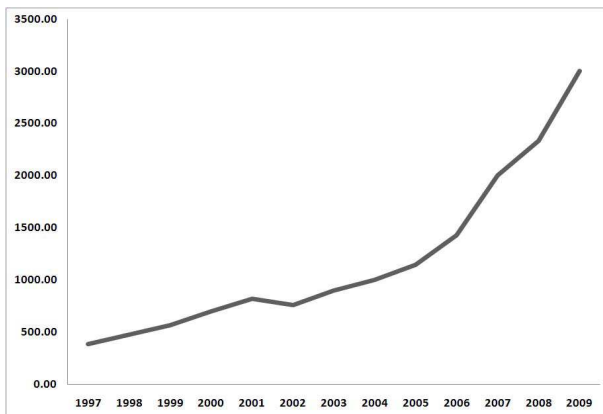


Figure 1: The total number of publications devoted to the heavy-tailed and power law distributions in the arXiv (<http://arxiv.org>) grows fast each year.

In this survey, we call a distribution *heavy-tailed* if it does not have the exponentially bounded asymptotes. Namely, given a random variable X characterized by the probability distribution function

$$F(x) = \Pr[x < X],$$

we say that it has a *heavy right tail* if

$$\lim_{x \rightarrow \infty} F(x) \cdot \exp \lambda x = \infty, \quad \forall \lambda > 0. \quad (1)$$

An important subclass of heavy-tailed distributions is the *sub-exponential* distributions [2], for which a sum of n independent random variables X_1, X_2, \dots, X_n , with common distribution $F(x)$ is given,

$$\Pr[x < X_1 + X_2 + \dots + X_n] \underset{x \rightarrow \infty}{\sim} \Pr[x < \max(X_1, X_2, \dots, X_n)]. \quad (2)$$

Among sub-exponential distributions, we shall be essentially interested in those distributions of a random variable X which are characterized by a *power law decay*,

$$\Pr[x < X] \underset{x \rightarrow \infty}{\sim} \frac{1}{x^{1+\gamma}}, \quad (3)$$

for some $\gamma > 0$.

There are several physical mechanisms known as underlying the power law behaviors. Power law distributions often manifest a form of regularity arising through growth processes which is composed of a large number of common events and a small number of rarer events happened randomly. As the number of events grows, their distribution, under certain conditions, might converge to

a steady state (3). The mechanism of *preferential attachment* in which some quantity is distributed at random among a number of individuals according to how much they already have had been proposed in [3] as an algorithm explaining power law degree distributions in some scale-free networks. Graphs in that grow by successively adding a new vertex say x at each time step that links to an already existing one of the degree k , with the probability $\propto k/N$ where N is the total number of vertices present in the graph. The preferential attachment process generates a heavy-tailed distribution following a power law in its tail.

Power laws are also found in the study of stochastic processes involving multiplicative noises [1]. A typical equation of multiplicative stochastic process is given by a linear *Langevin equation* with a randomly changing coefficient. The effect of such a random coefficient drastically enhance the additive random force in the Langevin equation and increase fluctuations. Following [4], let us consider temporal fluctuations for a simple discrete time version of the Langevin equation,

$$x(t+1) = b(t) \cdot x(t) + f(t), \quad (4)$$

where $f(t)$ represents a random additive noise, and $b(t)$ is a non-negative stochastic coefficient interpreted as dissipation for $b(t) < 1$ and amplification for $b(t) > 1$. If we assume for simplicity that $b(t)$ and $f(t)$ are independent white noises having stationary statistics, and $f(t)$ is symmetric, we obtain, for the second order moment,

$$\langle x^2(t+1) \rangle = \langle b^2 \rangle \langle x^2(t) \rangle + \langle f^2 \rangle, \quad (5)$$

in which the angular brackets denote an average over realizations. For constant b^2 and f^2 , there is a stationary solution,

$$\langle x^2 \rangle = \frac{\langle f^2 \rangle}{1 - \langle b^2 \rangle}, \quad \langle b^2 \rangle < 1, \quad (6)$$

but $\langle x^2(t) \rangle$ diverges as $t \rightarrow \infty$, for $\langle b^2 \rangle > 1$. The statistics of $x(t)$ is estimated theoretically by introducing the characteristic function,

$$\mathfrak{F}(\xi, t) = \langle e^{i\xi x(t)} \rangle. \quad (7)$$

When $\langle x^2(t) \rangle$ diverges, $\mathfrak{F}(\xi, t)$ has singularity at $\xi = 0$ in the limit of $t \rightarrow \infty$, so that Taylor expansion cannot be applied for the steady solution. In such a case the following fractional power term can be assumed for the lowest order term because the characteristic function is generally a continuous function

$$\mathfrak{F}(\xi, \infty) = 1 - \text{const} \cdot |\xi|^\beta + \dots, \quad 0 < \beta < 2, \quad (8)$$

which is equivalent to the assumption of power law tails for the cumulative probability distribution

$$\text{Pr}[|x| < X] \sim \frac{1}{x^\beta}. \quad (9)$$

The validation of stochastic mechanisms generating the power-law behavior remains an active field of research in many areas of modern science.

In the forthcoming sections, we consider in details other, more sophisticated mechanisms that might bring forth fat-tail statistics in dynamical systems.

The plan of our review is following. In Sec. 2, we discuss the Degree-Mass-Action principle in random graphs formation - the preferential attachments and their natural generalizations. In Sec. 3, we consider the statistics of bursts in systems close to a threshold of instability. Then, in Sec. 4, we review the emergence of fat tails in queuing systems. Finally, in Sec. 5, we explain the appearance of power law distributions in models of Self-Organized Criticality. We conclude in the last section.

2. Degree-Mass-Action principle in random graphs formation

Random graphs with scale-free probability degree distributions are ubiquitous while modeling many real world networks such as the World Wide Web, social, linguistic, citation and biochemical networks; an excellent survey is [5]. The preferential attachment principle, together with its various modifications, could be seen as a particular case of *degree-mass-action* principle since the degree of a node acts in that as a positive affinity parameter quantifying the attractiveness of the node for new vertices. Our first aim is to construct a family of static random graph models, in which vertex degrees are distributed power-law like, while edges still have high degree of independence. As usual in random graph theory, we will entirely deal with asymptotic properties in the sense that the graph size goes to infinity.

2.1. A random graph space of the preferential attachment model

We consider graphs with vertex set $V = V_n = \{1, \dots, n\}$ where an edge between the vertices x and y (denoted by $x \sim y$) is interpreted as a persistent contact between the two nodes. Given $x \in V$, its degree is denoted by $d(x)$.

We will think of edges as generated by a pair-formation process in which each vertex x - often denoted as an individual - chooses a set of partners according to a specified x -dependent rule. Therefore the set of individuals which have contact with a given vertex x can be divided into two -possible non-disjoint sets: the set of nodes which are chosen by x himself and the set of nodes which have chosen x as one of their partners. We call the size of the first set the out-degree $d_{out}(x)$ of x and the size of the second one the in-degree $d_{in}(x)$ of x . Obviously,

$$d(x) \leq d_{out}(x) + d_{in}(x), \quad (10)$$

and if the choices are sufficiently independent one can expect equality to hold almost surely if $n \rightarrow \infty$.

We partition the set of vertices V_n into groups $\{C_i(n)\}_{i \geq 1}$ where all members of a group $C_i(n)$ choose exactly i partners by themselves ($d_{out} = i$ on $C_i(n)$). Let $P_\alpha^1(n, j)$ the probability for x to choose a fixed partner $y \in C_j(n)$ if n partners are available for the choice and just one choice will be made be

$$P_\alpha^1(n, j) = A_\alpha(n) \frac{j^\alpha}{n} \quad (11)$$

Here $A_\alpha(n)$ is a normalization constant such that

$$A_\alpha(n) \left(\sum_{i \geq 1} |C_i(n)| \frac{i^\alpha}{n} \right) = 1$$

and α is a real parameter. Since we want

$$A_\alpha(n) \rightarrow_{n \rightarrow \infty} A_\alpha$$

we need $\sum_i |C_i(n)| \frac{i^\alpha}{n}$ to be bounded as a function of n which will impose later on constraints on the constant α . The parameter α acts as an affinity parameter tuning the tendency to choose a partner with a high out-degree or low out-degree. If $\alpha = 0$, choices are made without any preferences and $A_\alpha(n) \equiv 1$. For $\alpha > 0$ the "highly active" individuals are preferred whereas for $\alpha < 0$ the "low activity" individuals are favored. From this we obtain the basic probability

$$\Pr[x \sim y] \simeq A_\alpha(n) \frac{i \cdot j^\alpha}{n}, \quad x \in C_i, \quad y \in C_j. \quad (12)$$

Concerning the size of the sets $C_i(n)$ we will make the following assumption:

$$\frac{|C_i(n)|}{n} = p_i(n) \rightarrow_{n \rightarrow \infty} \frac{c_1}{i^\gamma}. \quad (13)$$

With this choice we have to impose the restriction $\alpha < \gamma - 1$ to ensure the convergence of $A_\alpha(n)$. We require furthermore $\gamma > 2$ throughout the paper since otherwise the expected in-degree for individuals from a fixed group would diverge. The basic probabilities together with the fixed out-degree distribution define a probability distribution on each graph with vertex-set V_n , and therefore a random graph space $\mathcal{G}_n(\alpha, \gamma)$.

First we want to compute the important pairing probabilities. We start with the easier case $\alpha = 0$.

$$\Pr(x \sim y \mid x \in C_i; y \in C_k) = \frac{i+k}{n} - \frac{ik}{n^2} \sim_{n \rightarrow \infty} \frac{i+k}{n} \quad (14)$$

Likewise one can compute the corresponding probabilities for $\alpha \neq 0$. Dropping the simple details we just state the result:

$$\Pr(x \sim y \mid x \in C_i; y \in C_k) \simeq A_\alpha \frac{(ki^\alpha + k^\alpha i)}{n}, \quad n \rightarrow \infty. \quad (15)$$

It turns out, that the typical graphs in this model still have for $\alpha < 2$ a *power-law* distribution for the degree with an exponent which can be different from the exponent of the out-degree.

For $\alpha > 2$ we obtain a degree distribution which follows in mean a power law but has gaps. To compare both domains we will use the integrated tail distribution

$$F_k = \Pr(d(x) > k).$$

We will show that in both cases we get the same integrated tail distribution. Since we are interested in the dependence of the epidemic threshold from the power-law exponent of the total degree distribution we have to analyze how this exponent varies with the two parameters α and γ . Since the partner choice is sufficiently random and not too strongly biased toward high degree individuals (that's the meaning of the condition $\alpha \leq \gamma - 1$) it is easy to see that the in-degree distribution of a vertex from group C_i converges for $n \rightarrow \infty$ to a Poisson distribution with mean $\text{const} \cdot i^\alpha$. There are essentially two regimes in the parameter space, one for which the expected in-degree is of smaller order than the out-degree over all groups and one where the in-degree is asymptotically of larger order. In the first case it is clear that the in-degree is too small to have an effect on the degree distribution exponent. In other words: the set of individuals with degree k consists mainly of individuals whose out-degree is of order k . An easy estimation using the formula for the pairing probabilities shows that the expected in-degree of individuals from group i is given by

$$\mathbb{E}(d_{in}(x) \mid x \in C_i) \simeq \text{const} \cdot i^\alpha$$

asymptotically. Therefore the in-degree is of smaller order than the out-degree if $\alpha < 1$. In the case $\gamma - 1 \geq \alpha \geq 1$ the set of individuals with degree k consists mainly of individuals from groups with an index of order $k^{1/\alpha}$.

2.2. The Cameo Principle. The origins of scale-free graphs in social networks.

In the present section, we describe an edge formation principle related upon a structure *a priori* imposed on the vertex set. We assume that such a structure can be specified by a real positive random variable $\omega \in \mathbb{R}^+$ that quantifies some social property of an individual such as its wealth, popularity, or beauty being distributed over the population with a given probability distribution $\varphi(\omega)$.

Furthermore, we assume that a link between the two individuals, x and y , arises as a result of a directed choice made by either x or y (symbolized by $x \rightarrow y$ or $y \rightarrow x$ respectively); in many real life networks edges are formed that way. Although the edge creation is certainly a directed process, in the present section we consider the resulting graph to be undirected since for the majority of relevant transmission processes defined on the network the original orientation of an edge is irrelevant.

We suppose that the pairing probability follows an *inverse mass-action-principle*: the probability that x decides to connect to y characterized by its affinity value $\omega(y)$ reads as

$$\Pr\{x \rightarrow y \mid \omega(y)\} \sim \frac{1}{N} \cdot \frac{1}{\varphi(\omega(y))^\alpha}, \quad \alpha \in (0; 1) \quad (16)$$

where N being the total number of vertices. Let us note that it is not the actual value $\omega(y)$ which plays a decisive role while pairing, but rather its relative frequency of appearance over the population. The proposed principle captures the essence of antiquity markets – the more rare a property is, the higher is its value, and the more attractive it becomes for others. The pairing probability model

described above had been introduced in [34] and called the *Cameo-principle* having in mind the attractiveness, rareness and beauty of the small medallion with a profiled head in relief called Cameo. And it is exactly their rareness and beauty which gives them their high value.

In the *Economics of Location theory* introduced by [6] and developed by [7], a city, or even more certainly, a particular district in that may specialize in the production of a good that can be connected with natural resources, education, policy, or just low salary expenditures. City districts compete among themselves in a city market not necessarily connected with the quantity of their inhabitants. The demand for these products comes into the city district from everywhere and can be considered as exogenous. Then, the local attractiveness of a site determining the creation of new spaces of motion in that is specified by a real positive random variable $\omega > 0$. Indeed, it is rather difficult if ever be possible to estimate exactly the actual value $\omega(i)$ for any site in the urban pattern, since such an estimation can be referred to both the economic and cultural factors that may vary over the different historical epochs and over the certain groups of population. In the framework of a probabilistic approach, it seems natural to consider the value ω as a real positive independent random variable distributed over the vertex set of the graph representation of the site uniformly in accordance to a smooth monotone decreasing probability density function $f(\omega)$.

While investigating the model of Cameo graphs, we assume that

- The parameter ω is independent identically distributed (i.i.d.) over the vertex set with a smooth monotone decreasing density function $\varphi(\omega)$
- Edges are formed by a sequence of *choices*. By a choice we mean that a vertex x chooses another vertex, say y , to form an edge between y and x . A vertex can make several choices. All choices are assumed to be independent of each other.
- If x makes a choice the probability of choosing y depends only on the relative density of $\omega(y)$ and is of the form (16).
- A pre-defined out-degree distribution determines the number of choices made by the vertices. The total number of choices (and therefore the number of edges) is assumed to be about $\text{const} \cdot N$.

We focus on the striking observation that under the above assumptions a scale-free degree distribution emerges independently of the particular choice of the ω -distribution. Furthermore, it can be shown that the exponent in the degree distribution becomes independent of $\varphi(\omega)$ if the tail of φ decays faster than any power law.

Let $V_N = \{1, \dots, N\}$ be the vertex set of a random graph space. We are mainly interested in the asymptotic properties for N being very large. We assign i.i.d. to each element x from the set V_N a continuous positive real random variable (r.v.) $\omega(x)$ taken from a distribution with density function $\varphi(\omega)$. The variable ω can be interpreted as a parametrization of V_N . For a set

$$C_{\omega_0, \omega_1} = \{x : \omega(x) \in [\omega_0, \omega_1]\}, \quad (17)$$

we obtain

$$\mathbb{E}(\#C_{\omega_0, \omega_1}) = N \cdot \int_{\omega_0}^{\omega_1} \varphi(\omega) d\omega \quad (18)$$

where $\#C_{\omega_0, \omega_1}$ denotes the cardinality of the set (17). Without loss of generality, we always assume that $\varphi > 0$ on $[0, \infty)$, and that the tail of the distribution for φ is a monotone function, namely that $\varphi \in C^2([0, \infty))$ and the second derivatives, $D^2(\varphi^\mu)$, have no zeros for $|\mu| \in (0, \mu_0)$ and $\omega > \omega_0(\mu)$.

Edges are created by a directed process in which the basic events are choices made by the vertices. All choices are assumed to be i.i.d. The number of times a vertex x makes a choice is itself a random variable which may depend on x . We call this r.v. $d_{out}(x)$. The number of times a vertex x was chosen in the edge formation process is called the in-degree $d_{in}(x)$. Each choice generates a directed edge. We are mostly interested in the corresponding undirected graph. If we speak in the following about out-degree and in-degree we refer just to the original direction in the edge formation process. Let

$$p_\omega = \Pr\{x \rightarrow y \mid \omega = \omega(y)\}$$

be the basic probability that a vertex y with a fixed value of ω is chosen by x if x is about to make a choice. For a given realization ξ of the r.v. ω over V_N we assume:

$$p_\omega(\xi, N) = \frac{1}{N} \cdot \frac{A(\xi, N)}{[\varphi(\omega)]^\alpha}. \quad (19)$$

where $\alpha \in (0, 1)$ and $A(\xi, N)$ is a normalization constant. It is easy to see that the condition

$$\int_0^\infty [\varphi(\omega)]^{1-\alpha} d\omega < \infty$$

is necessary and sufficient to get

$$A(\xi, N) \rightarrow A > 0,$$

for $N \rightarrow \infty$ where convergence is in the sense of probability. Therefore, we need $\alpha < 1$.

One might argue that the choice probabilities should depend more explicitly on the actual realization ξ of the r.v. ω over V_N -not only via the normalization constant. The reason not to do so is twofold. First it is mathematically unpleasant to work with the empirical distribution of ω induced by the realization ξ since one had to use a somehow artificial N -dependent coarse graining. Second the empirical distribution is not really "observed" by the vertices (having in mind for instance individuals in a social network). What seems to be relevant is more the common believe about the distribution of ω . In this sense our setting is a natural one.

The emergence of a power law distribution in the above settings is not a surprise as it might seem for the first glance. The situation is best explained by

the following example. Let us take

$$\varphi(\omega) = C \cdot e^{-\omega}$$

and define a new variable

$$\omega^* = \frac{1}{[\varphi(\omega)]^\alpha} = \frac{e^{\omega\alpha}}{C^\alpha}.$$

The new variable ω^* can be seen as the effective parameter to which the vertex choice process applies. What is the induced distribution of ω^* ? With

$$F(z) = \Pr\{\omega^* < z\}$$

we obtain

$$F(z) = \int_0^{\frac{1}{\alpha} \ln C^\alpha \cdot z} \varphi(\omega) d\omega = -\frac{1}{z^{1/\alpha}} - C, \quad (20)$$

and therefore the ω^* -distribution

$$\phi(\omega^*) = \frac{1}{\alpha} \cdot \frac{1}{(\omega^*)^{1+1/\alpha}}.$$

This is a power law distribution with an exponent depending only on α .

The detailed results on the degree-degree correlations, the clustering coefficients, and the second moment of degree distributions are discussed in [34].

3. The statistics of bursts in systems close to a threshold of instability

Systems driven by random processes at a threshold of stability may exhibit a random switching of a signal between a quiescent (stable) and a bursting (unstable) state. Such an *intermittent* behavior is observed over a broad class of different systems in physics and nonlinear dynamics. Depending on the origin, the intermittent behavior either meets the classification proposed by Pomeau-Manneville [9] (the I-III types intermittency) or fits the features of the crisis-induced intermittency [10]. In both cases, the parameters of the models are static. Another example of intermittent behavior, called *on-off intermittency* has been introduced in [11] and then observed numerically and experimentally, [12, 13, 14, 15, 16, 17, 18, 19, 20, 21, 23]. The mechanism for this intermittency type relies on a random forcing of a bifurcation parameter through a bifurcation point.

The ergodic properties of a system at the threshold of stability can be partially characterized by the distribution of the quiescent times (the durations of laminar phases) $P(t)$ where $t \in \mathbb{N}$. Indeed, a complete characterization of the statistical properties of the system will imply the knowledge of residence times distribution for all the regions of the phase space and not only of the laminar regions. However, the former is the first important statistical indicator of such

dynamics and this is a reason why we focus at the quiescent times distributions in the present study.

Depending on the particular type of intermittency exhibited by the system, the statistics of this distribution can asymptotically meet either exponential laws, or power laws of exponent γ . Particularly, the power-law statistics for the quiescent times distribution is claimed to be typical for the systems demonstrating the on-off type intermittency, and the value of exponent γ depends in general from the nonlinearity characteristic of the dynamical system considered [22]. For example, in the experiments with ion-acoustic instabilities in a laboratory plasma [23], due to nonlinear effects, the exponent of power law depends on the value of a control parameter.

In the present section, we discuss the net effect produced on the statistics of laminar phases by the stochastic fluctuations of a system state variable (a bifurcation parameter) near the fluctuating threshold of stability (a bifurcation point).

We do not refer to any definite physical system displaying an intermittent behavior. For the toy model which we introduce, the bifurcation parameter and the bifurcation point are considered as random independent variables. It is supposed that intermittency takes place in the system when the process crosses the threshold value.

The control parameter of the system is the number $\eta \in [0, 1]$, which represents a relative frequency of fluctuation of the threshold value: varying the parameter η amounts to modifying the relation between the characteristic time scales of the threshold variable and those of the state variable.

At $\eta = 0$ (when the state and the threshold variables have the same time scale) the statistics of laminar phases is exponential, while at $\eta = 1$ (the limiting case of quenched threshold) it can be power law; for the intermediate values $0 < \eta < 1$, the statistics is mixed becoming exponential for sufficiently large times.

In general, the statistics of laminar phases depends on the statistics of the random system state variable and threshold described by the probability distributions F and G respectively. For many distributions F and G , the proposed model can be solved analytically.

3.1. Systems at a threshold of instability

Let us suppose that the state of a system can be characterized by a real number $x \in [0, 1]$. Another real number $y \in [0, 1]$ plays the role of a threshold of stability. The system is stable as long as $x < y$ and exhibits a sudden transition to the irregular state otherwise ($x \geq y$).

We consider x as a random variable distributed with respect to some given probability distribution function

$$P\{x < u\} = F(u).$$

In an analogous way, the value of the threshold y is also a random variable distributed over the interval $[0, 1]$ with respect to some other probability distri-

bution function (pdf)

$$P\{y < u\} = G(u).$$

In general, F and G are two arbitrary left-continuous increasing functions satisfying the normalization conditions

$$F(0) = G(0) = 0, \quad F(1) = G(1) = 1.$$

Given a fixed real number $\eta \in [0, 1]$, we define a discrete time random process in the following way. At time $t = 0$, the variable x is chosen with respect to pdf F , and y is chosen with respect to pdf G . If $x \geq y$, the process continues and goes to time $t = 1$. At time $t \geq 1$, the following events happen:

i) with probability η , the random variable x is chosen with pdf F but the threshold y keeps the value it had at time $t - 1$. Otherwise,

ii) with probability $1 - \eta$, the random variable x is chosen with pdf F , and the threshold y is chosen with pdf G .

If $x \geq y$, the process ends; if $x < y$, the process continues and goes to time $t + 1$.

Eventually, at some time step t , when the state variable x exceeds the threshold value y , the process stops, and the system destabilizes, so this integer value $t = T$ acquired in this random process limits the duration of the episode of laminar dynamics. In the laps of time, the system regains the composure state, when $x < y$, and the process starts again.

While studying the above model, we are interested in the distribution of the duration of laminar phases $P_\eta(T; F, G)$ provided the probability distributions F and G are given and the control parameter η is fixed.

Even if in our model the state variable x is treated as a random variable, what is really important in what follows is the corresponding pdf F . It would in fact be possible to treat x as a deterministic dynamical variable defined by the iterated images of a map of the interval $[0, 1]$. In this case we would assume the existence of an invariant ergodic (Bernoulli) measure dF , for which x is a generic orbit.

It is also to be noticed that the model proposed resembles closely the coherent-noise models [25, 26] discussed in concern with a standard sandpile model [27] in self-organized criticality, where the statistics of avalanche sizes and durations take power-law forms. No exact analytical results concerning the coherent-noise models have been obtained so far. The proposed toy model has not been discussed in the literature before and, in principle, is much simpler than those discussed in [25, 26] since it does not involve any spatial dynamics typical of such extended systems with quenched memory as the original sandpile models.

3.2. Distribution of residence times below the threshold

We are interested in the probability $P_\eta(T; F, G)$ that the random process introduced in the previous section ends precisely at time T with a crossing of the threshold, provided the distributions F and G are given and η is fixed. We

shall denote $P_\eta(T; F, G)$ simply as $P(T)$. A straightforward computation shows directly from the definitions of Sec. 3.1 that

$$P(0) = \int_0^1 dG(y) (1 - F(y)). \quad (21)$$

For $T \geq 1$, the system can either stay below the threshold in the laminar state (a "survival") (S) or surmount the threshold to a burst state (a "death") (D). Both events can take place either in the correlated way (with probability η ; see (i) in Sec. 3.1) (we denote them S_c and D_c), or in the uncorrelated way (with probability $1 - \eta$; see (ii) in section Sec. 3.1) (S_u and D_u). For $T = 1$, we have for example

$$\begin{aligned} P(1) &= P[SD_c] + P[SD_u] \\ &= \eta \int_0^1 dG(y) F(y) (1 - F(y)) \\ &\quad + (1 - \eta) \int_0^1 dG(y) F(y) \int_0^1 dG(z) (1 - F(z)) \\ &= \eta B(1) + (1 - \eta) A(1) B(0). \end{aligned} \quad (22)$$

Similarly,

$$\begin{aligned} P(2) &= \eta^2 B(2) + \eta(1 - \eta) (A(1)B(1) + A(2)B(0)) \\ &\quad + (1 - \eta)^2 A(1)^2 B(0), \end{aligned} \quad (23)$$

where where we have defined, for $n = 0, 1, 2, \dots$,

$$A(n) = \int_0^1 dG(y) F(y)^n \quad (24)$$

and

$$\begin{aligned} B(n) &= \int_0^1 dG(y) F(y)^n (1 - F(y)) \\ &= A(n) - A(n + 1). \end{aligned} \quad (25)$$

It is useful to introduce the generating function of $P(T)$:

$$\hat{P}(s) = \sum_{T=0}^{\infty} s^T P(T).$$

The generating property of the function $\hat{P}(s)$ is such that

$$P(T) = \frac{1}{T!} \left. \frac{d^T \hat{P}(s)}{ds^T} \right|_{s=0}. \quad (26)$$

Defining the following auxiliary functions

$$\begin{aligned} p(l) &= \eta^l A(l + 1), & \text{for } l \geq 1, \quad p(0) &= 0, \\ q(l) &= (1 - \eta)^l A^{l-1}(1), & \text{for } l \geq 1, \quad q(0) &= 0, \\ r(l) &= \eta^l [\eta B(l + 1) + (1 - \eta) A(l + 1) B(0)], & \text{for } l \geq 1, \quad r(0) &= 0, \\ \rho &= \eta B(1) + (1 - \eta) A(1) B(0). \end{aligned} \quad (27)$$

we find

$$\hat{P}(s) = B(0) + \rho s + \frac{s[\hat{r}(s) + \rho\hat{p}(s)\hat{q}(s) + \rho A(1)\hat{q}(s) + A(1)\hat{q}(s)\hat{r}(s)]}{1 - \hat{p}(s)\hat{q}(s)}, \quad (28)$$

where $\hat{p}(s), \hat{q}(s), \hat{r}(s)$ are the generating functions of $p(l), q(l), r(l)$, respectively.

In the marginal cases of $\eta = 0$ and $\eta = 1$, the probability $P(T)$ can be readily calculated. For $\eta = 0$, equations (27) and (28) give

$$\hat{P}_{\eta=0}(s) = \frac{B(0)}{1 - sA(1)}. \quad (29)$$

Applying the inverse formula (26) to equation (29), we get

$$P_{\eta=0}(T) = A^T(1)B(0) = \left[\int_0^1 dG(y)F(y) \right]^T \int_0^1 dG(y)(1 - F(y)).$$

Therefore, in this case, for any choice of the pdf $F(u)$ and $G(u)$, the probability $P(T)$ decays exponentially.

For $\eta = 1$, equations (27) and (28) yield

$$\hat{P}_{\eta=1}(s) = \hat{B}(s), \quad (30)$$

so that

$$P_{\eta=1}(T) = B(T) = \int_0^1 dG(y)F(y)^T(1 - F(y)). \quad (31)$$

3.2.1. Some examples of decay in the correlated case $\eta = 1$

We have just seen that the probability $P(T)$ decays exponentially, in the uncorrelated case $\eta = 0$, for any choice of the pdf F and G .

In the correlated case $\eta = 1$, many different types of behavior are possible, depending on the form of the pdf F and G . We will examine an important class of F and G , for which $P_{\eta=1}(T)$ can be explicitly computed from equation (31). We will take F and G as absolutely continuous with respect to the Lebesgue measure, with

$$\begin{aligned} dF(u) &= (1 + \alpha)u^\alpha du, & \alpha > -1, \\ dG(u) &= (1 + \beta)(1 - u)^\beta du, & \beta > -1. \end{aligned} \quad (32)$$

Here we recognize the family of invariant measures of a map of the interval with a fixed neutral point [28].

Equation (31) gives in this case:

$$P_{\eta=1}(T) = \frac{\Gamma(2 + \beta)\Gamma(1 + T(1 + \alpha))}{\Gamma(2 + \beta + T(1 + \alpha))} - \frac{\Gamma(2 + \beta)\Gamma(1 + (T + 1)(1 + \alpha))}{\Gamma(2 + \beta + (T + 1)(1 + \alpha))}.$$

Using Stirling's approximation, we get for $T \gg 1$:

$$P_{\eta=1}(T) = \frac{(1 + \beta)\Gamma(2 + \beta)(1 + \alpha)^{-1 - \beta}}{T^{2 + \beta}} \left(1 + o\left(\frac{1}{T}\right) \right). \quad (33)$$

For different values of β , the exponent of the threshold distribution, we get all possible power law decays of $P_{\eta=1}(T)$. Notice that the exponent $(-2 - \beta)$ characterizing the decay of $P_{\eta=1}(T)$ is independent of the distribution F of the state variable.

We were not able to prove that the asymptotic decay of $P_{\eta=1}(T)$ is algebraic for any choice of the distributions F and G ; nevertheless, we have not found any counterexample contradicting this conjecture. Let us consider in particular the case of uniform F (the results of this section suggest in fact that what determines the decay of $P(T)$ is mostly the threshold pdf G): $P_{\eta=1}(T)$ is then a particular case of a Riemann-Liouville integral, and we did not find any case of non-algebraic decay for large T in the tables [29].

3.2.2. Upper and lower bounds for $P(T)$ for any η

We will use the fact that

$$A(1)^n \leq A(n) \leq A(1) \quad \text{and} \quad 0 \leq B(n) \leq A(1), \quad n = 1, 2, \dots \quad (34)$$

The upper bound for $A(n)$ is trivial, since $0 \leq F(y) \leq 1$ for any $y \in [0, 1]$. The lower bound is a consequence of Jensen's inequality, and of the fact that the function $x \rightarrow x^n$ is convex on the interval $]0, 1[$ for any integer n .

We now replace these bounds for $A(n)$ and $B(n)$ in the general formula for $P(T)$ and the resulting expressions in all the terms of the sums, except the one corresponding to the index $n = 0$ in $P_I(T)$. (This term, which corresponds to a sequence of correlated survivals, has to be treated separately, in order not to lose information on the case $\eta = 1$.) Labelling by the index k the number of uncorrelated survivals in the sequence of events considered in the sum for $P(T)$, we get

$$\begin{aligned} P_\eta(T) &\leq [\eta^T B(T) + \eta^{T-1}(1-\eta)A(T)B(0)] \\ &+ [\eta A(1) + (1-\eta)A(1)B(0)] \sum_{k=1}^{T-1} \gamma_k^{T-1} [(1-\eta)A(1)]^k \eta^{T-1-k} \end{aligned} \quad (35)$$

and

$$\begin{aligned} P_\eta(T) &\geq [\eta^T B(T) + \eta^{T-1}(1-\eta)A(T)B(0)] \\ &+ (1-\eta)A(1)B(0) \sum_{k=1}^{T-1} \gamma_k^{T-1} [(1-\eta)A(1)]^k \eta^{T-1-k} \end{aligned} \quad (36)$$

where γ_k^{T-1} represents the number of sequences of $T-1$ events c, u ($c =$ correlated survival, $u =$ uncorrelated survival) containing a number k of events u , so that

$$\gamma_k^{T-1} = \binom{T-1}{k}.$$

This implies the upper bound

$$\begin{aligned} P_\eta(T) &\leq \eta^T B(T) + (1-\eta)A(1)B(0) [\eta + (1-\eta)A(1)]^{T-1} \\ &+ \eta A(1) \left\{ [\eta + (1-\eta)A(1)]^{T-1} - \eta^{T-1} \right\} \end{aligned} \quad (37)$$

and the lower bound

$$\begin{aligned} P_\eta(T) &\geq \eta^T B(T) + (1 - \eta)A(1)^T B(0) \\ &= \eta^T P_{\eta=1}(T) + (1 - \eta)P_{\eta=0}(T). \end{aligned} \quad (38)$$

We thus see that, for any $0 \leq \eta < 1$, the decay of distribution $P(T)$ is bounded by exponentials. Furthermore, the bounds (37) and (38) are exact in the marginal cases $\eta = 0$ and $\eta = 1$.

3.2.3. Behavior of $P(T)$ for intermediate times

We have seen in Sec. 3.2.1 that there exists a class of pdfs for which $P_\eta(T)$ decays like a power law when $\eta = 1$. In section 3.2.2, we show that for any $\eta < 1$ the asymptotic decay of $P_\eta(T)$ is exponential. We now make some remarks about the behavior of $P_\eta(T)$ for η close to 1. The first thing to be noted is that, for T fixed, $P_\eta(T)$ is a continuous function of η , since it is a finite sum of continuous functions (see Sec. 3.2.2). This results, of course, imply that the continuity cannot be uniform in T . This means that, for any fixed interval of times $[T_-, T_+]$, with T_- in the range of validity of the power-law asymptotes (33) of $P_1(T)$, $P_\eta(T)$ will be arbitrarily close to the same power law for η sufficiently close to 1. For times $T \gg T_+$, the decay becomes exponential. We shall see in the next section that for the case of uniform densities, it is possible to estimate the value of the crossover time to the exponential behavior as a function of η .

3.3. Distribution of quiescent times for the case of uniform densities

In this section, we consider the distribution of quiescent times for the special case of uniform densities $dF(u) = dG(u) = du$, for all $u \in [0, 1]$ and for any $\eta \in [0, 1]$. In this case, simpler and implicit expressions can be given for $\hat{P}(s)$ and $P(T)$. After some tedious but trivial computation, we get from equation (28):

$$\hat{P}(s) = \frac{1}{1 + (1 - \eta)\gamma(s)} \left[\frac{1 + \gamma(s)}{s} - \eta\gamma(s) \right], \quad (39)$$

where $\gamma(s)$ is defined by

$$\gamma(s) = \frac{\ln(1 - \eta s)}{\eta s}. \quad (40)$$

The asymptotic behavior of $P(T)$ is determined by the singularity of the generating function $\hat{P}(s)$ that is closest to the origin.

For $\eta = 0$, the generating function has a simple pole $\hat{P}(s) = (2 - s)^{-1}$, and therefore $P(T)$ decays exponentially, which agrees with the result of the previous section. In Fig. 3.3, we have presented the distribution of quiescent times $P(T)$ in log-linear scale for $\eta = 0$.

For the intermediate values $1 > \eta > 0$, the generating function $\hat{P}(s)$ has two singularities. One pole, $s = s_0$, corresponds to the vanishing denominator $1 + (1 - \eta)\gamma(s)$, where s_0 is the unique nontrivial solution of the equation

$$-\ln(1 - \eta s) = s \frac{\eta}{1 - \eta}. \quad (41)$$

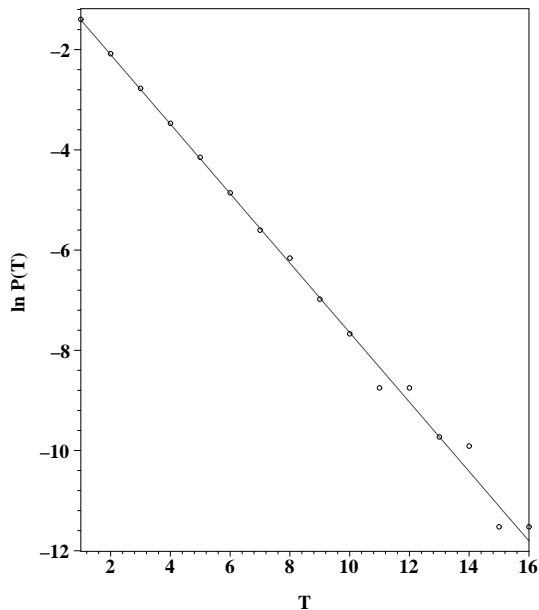


Figure 2: Distribution of quiescent times for the uniformly distributed variables x and y . $P_\eta(T)$ decays exponentially for $\eta = 0$, consistently with the analytical result $P(T) = 2^{-(T+1)}$ (solid line).

Another singularity, $s = s_1 = \eta^{-1}$, corresponds to the vanishing argument of the logarithm. It is easy to see that $1 < s_0 < s_1$, so that the dominant singularity of $\hat{P}(s)$ is of polar type, and the corresponding decay of $P(T)$ is exponential, with rate $\ln(s_0(\eta))$, for times much larger than the crossover time $T_c(\eta) \sim \ln(s_0(\eta))^{-1}$.

The results of Sec. 3.2.2 about the upper bound for the distribution $P(T)$ allow us to be more precise about this decay rate. In particular, since $B(T) \leq A(1)$, it follows from (37) that

$$P(T) \leq \frac{\eta A(1) + (1 - \eta)A(1)B(0)}{(\eta + (1 - \eta)A(1))^{T-1}} \quad (42)$$

which in the case of uniform densities gives

$$P(T) \leq \frac{1}{2} \left(\frac{1 + \eta}{2} \right)^T. \quad (43)$$

We have then

$$\frac{1}{s_1} = \eta < \frac{1}{s_0} \leq \frac{1 + \eta}{2} \quad (44)$$

and we see that the rate $\ln(s_0(\eta))$ vanishes like $1 - \eta$ as η tends to 1.

When η tends to 1, the two singularities s_0 and s_1 merge. More precisely, we have

$$\hat{P}_{\eta=1}(s) = \frac{s + (1 - s) \ln(1 - s)}{s^2}. \quad (45)$$

The corresponding dominant term in (45) is of order $O(T^{-2})$ [30]. This obviously agrees with the exact result we get from equation (31), with $dF(u) = dG(u) = du$:

$$P_{\eta=1}(T) = \frac{1}{(T+1)(T+2)} . \quad (46)$$

In Fig. 3.3, we have drawn the distribution of quiescent times $P_{\eta=1}(T)$ that exhibits the power-law decay, with the slope $\gamma = -2$.

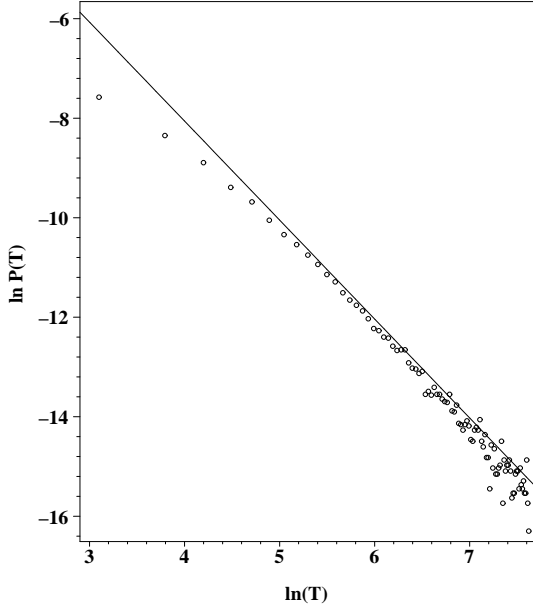


Figure 3: Distribution of quiescent times for the uniformly distributed variables x and y . We show the power-law decay of $P_{\eta=1}(T)$ plotted in the log-log scale. The solid line is given by (46).

In the case of uniform densities, it is possible to get an expression of $P(T)$ for all times, and for any value of η , by applying the inversion formula (26) to (39):

$$P(T) = \frac{\eta^T}{(T+1)(T+2)} + \sum_{k=1}^T \frac{\eta^T}{(T-k+1)(T-k+2)k} \sum_{m=1}^k \left(\frac{1-\eta}{\eta}\right)^m c(m, k) , \quad (47)$$

where $c(m, k)$ is defined by

$$c(m, k) = m! \sum_{\substack{l_1+l_2+\dots+l_m=k \\ l_i \geq 1}} \frac{l_1 l_2 \dots l_{m-1} l_m}{(l_1+1)(k-l_1)(l_2+1)(k-l_1-l_2) \dots (l_{m-1}+1)(k-l_1-l_2-\dots-l_{m-1})(l_m+1)} .$$

When $\eta \neq 0$, there is an alternative way of writing the previous expression:

$$P(T) = \frac{\eta^T}{(T+1)(T+2)} + \sum_{k=1}^T \frac{\eta^{T+1}}{(T-k+1)(T-k+2)} \sum_{l=1}^{\infty} (1-\eta)^l b(l, k), \quad (48)$$

where $b(l, k)$ is defined by

$$b(l, k) = \sum_{\substack{i_1+i_2+\dots+i_l=k \\ i_j \geq 0}} \frac{1}{(i_1+1)(i_2+1)\dots(i_{l-1}+1)(i_l+1)}.$$

In Fig. 3.3, we have plotted the distribution of quiescent times $P_\eta(T)$ for the intermediate values $\eta = 0.5$, $\eta = 0.7$, $\eta = 0.9$, together with the analytical result (47).

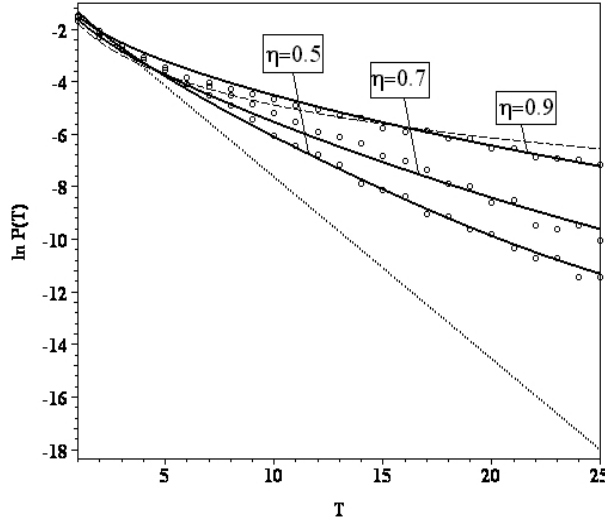


Figure 4: Distribution of quiescent times for the uniformly distributed variables x, y at the intermediate values $\eta = 0.5$, $\eta = 0.7$, $\eta = 0.9$ (circles). For comparison, the dotted line 2^{-T-1} presents the exponential decay for $\eta = 0$, and the dashed line corresponds to $1/(T+1)(T+2)$ for $\eta = 1$, see (46). The solid line is given by (47) for $\eta = 0.5$, $\eta = 0.7$, $\eta = 0.9$.

Note that in Fig. 3.3 and Fig. 3.3 (where $\eta \neq 1$), we only plot distributions $P(T)$ up to relatively short quiescent times ($T = 16$, $T = 25$), since these times are already greater than the crossover time $T_c(\eta) \sim 1/\ln(s_0)$ to the exponential decay $\exp(-\ln(s_0)T)$ (s_0 defined by equation (41)). For much longer times, very few survivals are observed, and the statistics gets bad. Of course, $T_c(\eta)$ grows as the parameter η tends to 1, so that we have good statistics for longer and longer times (in Fig. 3.3, for $\eta = 1$, the plot is for quiescent times $20 \leq T \leq 2000$).

A natural question arising in this context is about the relationship between the ergodic invariants that quantify the dynamics of deterministic systems, for example the Lyapunov exponents, and the scaling laws. The corresponding question for models of self-organized criticality is certainly also pertinent since in that case a relation is known between the Lyapunov spectrum and the transport properties [31]. In our case, however, because of the dynamical character not only of the state variable but also of the threshold, some extension of the definition of the invariants would be needed, which is beyond the scope of our discussion.

4. Fat tails in queuing systems

In a simplified model of human activity, [33, 47, 48], it is viewed as a decision based *queuing system* (QS) where tasks to be executed arrive randomly and accumulate before a server \mathcal{S} . Under the priority-based scheduling rules, in which each incoming task is endowed with a *priority index* (PI) indicating the urgency to process the job, the timing of the tasks follows fat tails probability distribution, (i.e the activity of the server exhibits bursts separated by long idle periods with the ubiquitous Poisson behavior).

There are two types of dynamics:

- i). *Service policies based on fixed priority indexes.* This case which is considered in [33, 47, 48] assumes that the value a of the PI is fixed once for all. Accordingly, very low priority jobs are likely to never be served. To circumvent this difficulty [33, 47, 48] introduce an ad-hoc probability factor $0 \leq p \leq 1$ in terms of which the limit $p \rightarrow 1$ corresponds to a deterministic scheduling strictly based on the PI's while in the other limit $p \rightarrow 0$ the purely random scheduling is in use.

In this setting, the *waiting time distribution* (WTD) of the tasks before service is shown to asymptotically exhibit a fat tail behavior. The main point of the Barabasi's contribution is to show that PI-based scheduling rules can alone generate fat tails in the WTD of unprocessed jobs.

- ii). *Service policies based on time-dependent priority indexes.* Here the priority index is time-dependent. This typically models situations where *the urgency to process a task increases with time* and $a(t)$ will hence be represented by increasing time functions.

Clearly, scheduling rules based on such a time-dependent PI do offer new specific dynamical features. They are directly relevant in several contexts such as:

- a). *Flexible manufacturing systems with limited resource.* Here a single server is conceived to process different types of jobs but only a single type can be produced at a given time t (i.e. this is the limited

resource constraint). Accordingly, the basic problem is to dynamically schedule the production to optimally match random demand arrivals for each types of items. The dynamic scheduling can be optimally achieved by using time-dependent priority indexes (*the Gittins' indexes*) which specify in real time, which type of production to engage [40]. Problems of this type belong to the wider class referred as the *Multi-Armed Bandit Problems* in operations research.

b). *Tasks with deadlines.* This situation, can be idealized by a queuing system where each incoming item has a deadline before which it definitely must be processed, [43, 44, 39]. In this case, to be later discussed in the present paper, we can explicitly derive the lead-time profile of the waiting jobs obtained under several scheduling rules, including the (optimal) time-dependent priority rule known as the *earliest-deadline-first* policy.

c). *Waiting time-dependent feedback queuing systems.* In queuing networks, priority indexes based on the waiting times can be used to schedule the routing through the network. For networks with loops, such scheduling policies are able to generate generically stable oscillations of the populations contained in the waiting room of the queues, [41].

In the context of QS, the *waiting time probability distribution* (WTD), (i.e. the time the tasks spend in the queue before being processed) is a central quantity to characterize the dynamics. It strongly depends on the arrival and service stochastic processes - in particular to the distributions of the *inter-arrival* and *service* time intervals. The first moments of these distributions, enable to define the traffic load

$$\rho = \frac{\lambda}{\mu} \geq 0,$$

(i.e. the ratio between the mean service time $1/\mu$ and the mean arrival time $1/\lambda$) and clearly the stability of elementary QS is ensured when $0 \leq \rho < 1$. Focusing on the WTD, [33, 47, 48] emphasized that heavy tails in the WTD can have several origins, three of which are listed below:

- 1). the *heavy traffic load of the server* which induces large "bursty" fluctuations in both the WTD and the busy period (BP) of the QS. For QS with feedback control driving the dynamics to heavy traffic loads, this allows to generate self-organized critical (SOC) dynamics, [34] and the resulting fat tails distribution exhibit a decay following a $-3/2$ exponent.
- 2). the presence of *fat tails in the service time distribution* produce fat tails of the WTD a property which is here independent of the scheduling rule [36]. For the convenience of the reader, we give here a short review of these results.
- 3). priority index scheduling rules as discussed in [33, 47, 48].

In this section we pay the essential attention to the case iii) but contrary to the discussion carried in [33, 47, 48], we shall here consider the dynamics in presence of *age-dependent priority indexes*. As it could have been expected, these aging mechanisms generate new behaviors that will be explicitly discussed for two classes of models.

4.1. Waiting time distributions for queuing systems with fat tail service times

Let us reproduce here a result recently derived in [36].

Theorem 4.1 (Boxma). *Assume that the (random) service time in a M/G/1 QS is drawn from a PDF with a regularly varying tail at infinity with index $\nu \in (-1, -2)$, (regularly varying with index $\nu \in (-1, -2) \Rightarrow$ fat tail with index $\nu \in (-1, -2)$). For this range of asymptotic behaviors of the PDF, the first moment β of the service exists.*

Assume further that the service is delivered according to a random order discipline. Then the waiting time distribution W_{ROS} exhibits a fat tail with index $(1 - \nu) \in (-1, 0)$ and more precisely, we can write

$$\Pr(W_{\text{ROS}} > x) \propto C \frac{\rho}{1 - \rho} \frac{h(\rho, \nu)}{\beta \Gamma(2 - \nu)} x^{1 - \nu} \mathcal{L}(x), \quad (49)$$

where $\rho < 1$ is the traffic intensity, β the average service time, $\mathcal{L}(x)$ a slowly varying function and

$$h(\rho, \nu) = \int_0^1 f(u, \rho, \nu) du,$$

with:

$$f(u, \rho, \nu) = \frac{\rho}{1 - \rho} \left(\frac{\rho u}{1 - \rho} \right)^{\nu - 1} (1 - u)^{1/(1 - \rho)} + \left(1 + \frac{\rho}{1 - \rho} \right)^{\nu} (1 - u)^{1/(1 - \rho) - 1}.$$

The fat tail behavior given in (49) is therefore entirely inherited from the fat tail behavior of the service and is not affected by any reduction of the traffic intensity ρ . Note also that change of the scheduling rule cannot get rid of this fat tail behavior. This point can be explicitly observed in [38, 45], who show that for the previous M/G/1 QS with a random order service (ROS) service discipline, one obtains:

$$\Pr(W_{\text{ROS}} > x) \propto_{x \rightarrow \infty} h(\rho, \nu) \cdot \Pr(W_{\text{FCFS}} > x), \quad (50)$$

from which we directly observe that *the fat tail in the asymptotic behavior is not altered by a change of the scheduling rule.*

Note finally that for the M/M/1 QS, (i.e. exponential service distributions and hence no fat tail), [42] shows that the random order service scheduling rule yields:

$$\Pr(W_{\text{ROS}} > x) \propto_{x \rightarrow \infty} C_{\rho} x^{-5/6} e^{-\gamma x - \delta x^{1/3}}, \quad (51)$$

with

$$C(\rho) = 2^{2/3} 3^{-1/2} \pi^{5/6} \rho^{17/12} \frac{1 + \rho^{1/2}}{[1 - \rho^{1/2}]^3} \exp \left\{ \frac{1 + \rho^{1/2}}{1 - \rho^{1/2}} \right\},$$

and

$$\gamma = \left(\rho^{-1/2} - 1 \right)^2 \quad \text{and} \quad \delta = 3 \left[\frac{\pi}{2} \right]^{2/3} \rho^{-1/6},$$

which has to be compared with the FCFS scheduling discipline, which for the same $M/M/1$ QS reads as, [38]:

$$\Pr(W_{\text{FCFS}} > x) = \frac{1}{\beta} (1 - \rho) e^{-(1-\rho)x/\beta}. \quad (52)$$

While the detailed behaviors given by (51) and (52) clearly differ, they however both share, in accord with [33], an exponential decay.

4.2. Scheduling based on time dependent priority indexes

The most naive approach to discuss the dynamics of QS with scheduling based on *time-dependent priority indexes* is to think of a population model in which the members suffer aging mechanisms which ultimately will kill them.

Naively, we may consider the population of a city in which members are either born in the city or immigrate into it at a certain age and finally die in the city. Assuming that the death probability *depends on each individual age*, the study of the age structure of the population exhibits some of the salient features of our original QS.

First, we discuss this class of models and then return to the original model of L. Barabási [33] to consider a simple QS where each task waiting to be processed carries a deadline (playing the role of a PI) and as time flows the these deadlines steadily reduce - this implies a (*time dependence of the PI*). At a given time, the scheduling of the tasks follows the "earliest-deadline-first" (EDF) policy and given a queue length configuration, we shall discuss the lead-time (lead-time = deadline - current time) profile of the tasks waiting to be served.

4.2.1. Tasks population dynamics with time dependent priority indexes

Consider a population of tasks waiting to be processed by \mathcal{S} with the following characteristics:

- i). An inflow of new tasks steadily enters into the queuing system. Each tasks is endowed with a priority index (PI) a which indicates its degree of urgency to be processed. In general, the tasks are heterogenous as the PI are different. In the time interval $[t, t + \Delta t]$, the number of incoming jobs exhibiting an initial PI in the interval $[a, a + \Delta a]$ is characterized by $G(a, t) \Delta t \Delta a$.

ii). Contrary to the situations discussed in [33], an "aging" process directly affects the urgency to process a given task. In other words the priority index a is not frozen in time but $a = a(t)$ monotonously increases with time t . For an infinitesimal time increase Δt , in the simplest case we shall have

$$a(t + \Delta t) = a(t) + \Delta t.$$

Here we slightly generalize this and allow inhomogeneous aging rates written as $p(a) > 0$ meaning that

$$a(t + \Delta t) = a(t) + p(a)\Delta t.$$

iii). The scheduling policy depends on the PI of the tasks in the queue and we will focus on the natural policy "*process the highest PI first*".

iv). at time t , a scalar field $M(a, t)$ counts the number of waiting tasks with priority index a . Hence $M(a, t)\Delta a$ is the number with PI $p(a) \in [a + \Delta a]$. Accordingly, the total workload facing the human server \mathcal{S} will be given, at time t by:

$$L(t) = \int_0^\infty M(a, t) da. \quad (53)$$

v). In the time interval $[t, t + \Delta t]$, the server \mathcal{S} processes tasks with an a -dependent rate $\mu(a)\Delta t$. Typically $\mu(a)$ could be a monotonously increasing function of a . As the service rate $\mu(a)$ explicitly depend on the PI a , it therefore plays an effective role of service discipline.

The previous elementary hypotheses imply an evolution in the form:

$$M(a + p(a)\Delta t, t + \Delta t)\Delta a \approx M(a, t)\Delta a - \mu(a)M(a, t)\Delta a\Delta t + G(a, t)\Delta t\Delta a.$$

Dividing by $\Delta a\Delta t$, we end, in the limits $\Delta a \rightarrow 0$ and $\Delta t \rightarrow 0$, with the scalar linear field equation:

$$\frac{\partial}{\partial t}M(a, t) + p(a)\frac{\partial}{\partial a}M(a, t) + \mu(a)M(a, t) = G(a, t). \quad (54)$$

It is worth to remark that the dynamics given by (54) is closely related to the famous McKendrick's age structured population dynamics, [37].

Assuming stationarity for the incoming flow of tasks (i.e. $G(a, t) = G_s(a)$), the linearity of (54) enables to explicitly write its stationary solution as:

$$M(a) = \pi(a) \left[C + \int_0^a \frac{G_s(z)}{p(z)\pi(z)} dz \right], \quad (55)$$

where

$$\pi(z) = \exp \left\{ - \int^z \frac{\mu(y)}{p(y)} dy \right\}, \quad (56)$$

with an integration constant $C < \infty$ remaining yet to be determined. Assume that the PI attached to the incoming jobs do not exceed a limiting value T , namely:

$$G(a, t) = \mathbb{I}(a < T) \hat{G}(a, t) \quad \Rightarrow \quad G_s(a) = \mathbb{I}(a < T) \hat{G}_s(a), \quad (57)$$

where $\mathbb{I}(a < T)$ is the indicator function. In other words (57) indicates that the new coming jobs do not exhibit arbitrarily high PI's.

This enables to define:

$$\Psi(T) = \int_0^\infty \frac{G_s(z)}{p(z)\pi(z)} dz = \int_0^T \frac{\hat{G}_s(z)}{p(z)\pi(z)} dz \quad (58)$$

and (55) reads as:

$$M(a) = \begin{cases} \pi(a) \left[C + \int_0^a \frac{\hat{G}_s(z)}{p(z)\pi(z)} dz \right] & \text{if } a \leq T \\ \pi(a) [C + \psi(T)] & \text{if } a > T. \end{cases} \quad (59)$$

The asymptotic behavior of $M(a)$ for $a \rightarrow \infty$ is entirely due to $\pi(a)$, (the square bracket terms are bounded by constants) and therefore (56) and (59) imply:

$$M(a) \approx \pi(a) \approx \begin{cases} e^{-k/qa^q} & \text{when } \frac{\mu(a)}{p(a)} \propto ka^{q-1}, \quad q > 0, \\ a^{-k} & \text{when } \frac{\mu(a)}{p(a)} \propto k/a, \end{cases} \quad (60)$$

In view of (60), the following alternatives occur:

a). For $q < 0$, in (60), the integral $\int_0^\infty M(z) dz$ does not exist. In this case an ever growing population of tasks accumulates in front of the server and the queuing process is exploding.

b). For $q > 0$, a stationary regime exists and in this case the constant $C < \infty$ in (59) can be determined by solving:

$$\int_0^\infty G_s(z) dz = \int_0^\infty M(z)\mu(z) dz, \quad (61)$$

which expresses a global balance between the stationary incoming and out going flows of tasks.

c). For $q = 0$ which implies that

$$\frac{\mu(a)}{p(a)} \propto \frac{k}{a},$$

(60) produces an exponent- k fat tail distribution for $M(a)$ counting the number of waiting tasks with PI a in the system. For $T < \infty$ and $a \rightarrow \infty$, the fat tail of $M(a)$ is populated by long waiting tasks i.e. those having spent more than $a - T$ waiting inside the system before being served. In the limiting case, for which

$$\mu(a) = \mu = \text{const}$$

and $p(a) = a$ (i.e. aging directly proportional to time) which leads to $q = 0$ in (60), the density $M(a)$ coincides directly with the WTD for $a \rightarrow \infty$.

This population model shares several features with the Barabási's model [33], namely:

- a). When a stationary regime exists, the function $\hat{G}_s(a)$ which here plays the role of the initial PI distribution in [33, 47, 48], does not affect the tail behavior given by (60).
- b). The scheduling rule here is implicitly governed by the service rate $\mu(a)$ which itself depend on time as the PI $a = a(t)$ are time-dependent. Note that $\mu(a)$ directly influences the asymptotic behavior of (60). In particular for case c), the tail exponent explicitly depends on $\mu(a)$.

Besides the similarities, we now also point out the important differences between the present population model and the model discussed in [33, 47, 48]:

- a) the service is not restricted to a single task at a given time (i.e. the service resource is not limited). Indeed $\mu(a)$ describes an average flow of service and hence several tasks can be processed simultaneously - (in the city population model the service corresponds to death and several individual may die simultaneously).
- b) while the fat tail in [33, 47, 48] is entirely due to the scheduling rule and therefore occurs even for QS far from traffic saturation, this is not so in the population model. Indeed in this last case, fat tails are due to heavy traffic loads occurring when the flow of incoming tasks nearly saturates the server, (this is implied by $q = 0$ in(60)) - for lower loads occurring when $q > 0$ the fat tail in (60) disappears.

4.2.2. Stochastic dynamics. Real-time queuing dynamics

In this section we will use the results of the real-time queuing theory (RTQS), pioneered in [43], to explore situations where the incoming jobs have a deadline - this problem is already suggested in [33]. Based on [43, 44, 32] and [39], first recall the basic hypotheses and the relevant results of RTQS's. Consider a general single server QS with arrival and service being described by independent renewal processes with average $1/\lambda$ respectively $1/\mu$ and finite variances for both

renewal processes. Each incoming task arrives with a random hard time relative deadline \mathcal{D} drawn from a PDF $G(x)$ with a density $g(x)$:

$$\Pr \{0 \leq \mathcal{D} \leq x\} = G(x),$$

with average $\langle \mathcal{D} \rangle$:

$$\langle \mathcal{D} \rangle = \int_0^\infty (1 - G(x)) dx = \int_0^\infty xg(x)dx.$$

At a given time t , we define the lead time \mathcal{L} to be given by:

$$\mathcal{L} = \mathcal{D} - t, \quad (62)$$

Assume now that the lead time \mathcal{L} plays the role of a priority index and the service is delivered by using the *earliest-deadline-first* (EDF) rule with preemption (i.e. the server always processes the job with the shortest lead time \mathcal{L}). Preemption implies that whenever an incoming job exhibits a shorter \mathcal{L} than the one currently in service, this incoming job is processed before, (i.e. *pre-empts*), the currently engaged task which service is postponed. The EDF rule directly corresponds to the deterministic policy (i.e. $p = 0, \gamma = 0$ in the original Barabási's contribution [33]).

At a given time, one can define a probability distribution corresponding to the *lead time profile* (LTP),

$$F(x) = \Pr \{-\infty \leq \mathcal{L} \leq x\},$$

of the jobs waiting in the QS. The LTP specifies the repartition of tasks having a given \mathcal{L} at time t . Knowing the queuing population Q at a given time, it is shown in [39] that for heavy traffic regimes, the LTP can, in a first order approximation scheme, expressed by a simple analytical form. Indeed, following [39], let us define the frontier $\hat{\mathcal{F}}(Q) > 0$ as the unique solution of the equation

$$\frac{Q}{\lambda} = \int_{\hat{\mathcal{F}}(Q)}^\infty (1 - G(x)) dx, \quad x \in [l, \infty) \subset \mathbb{R}^+. \quad (63)$$

Let us also define the frontier $\mathcal{F}(Q)$ as

$$\mathcal{F}(Q) = \begin{cases} \hat{\mathcal{F}}(Q) & \text{when } Q \leq Q^*, \\ \left(\langle \mathcal{D} \rangle - \frac{Q}{\lambda} \right) \leq l & \text{when } Q > Q^*, \end{cases} \quad (64)$$

with Q^* being defined by $\hat{\mathcal{F}}(Q) = l$ where l defined in (63).

In [39], it is shown that two alternative regimes can occur:

a) *Jobs served before deadline.* When $\langle \mathcal{D} \rangle > Q/\lambda$ and therefore $\hat{\mathcal{F}}(Q) = \mathcal{F}(Q)$, the LTP cumulative distribution $F(x)$ takes the form (see Fig. 5)

$$F(x) = \begin{cases} 0 & \text{when } x < \mathcal{F}(Q), \\ 1 - \frac{\lambda}{Q} \left(\int_x^\infty [1 - G(\eta)] d\eta \right) & \text{when } 0 < \mathcal{F}(Q) \leq x. \end{cases} \quad (65)$$

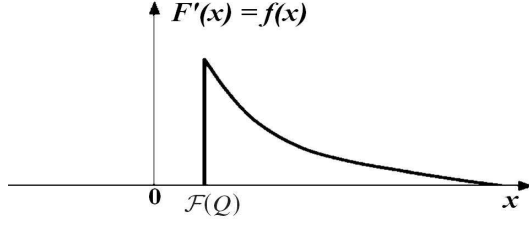


Figure 5: Density of the lead time profile $f(x) = dF(x)/dx$ when $F(Q) > 0$.

b) *Jobs served after deadline.* When $F(Q) = (\langle \mathcal{D} \rangle - Q/\lambda) \leq 0$, the LTP cumulative distribution $F(x)$ takes the form (Fig. 6)

$$F(x) = \begin{cases} 0, & \text{when } x < \langle \mathcal{D} \rangle - \frac{Q}{\lambda} < 0, \\ \left[1 + \frac{\lambda}{Q} (x - \langle \mathcal{D} \rangle) \right] \frac{Q - \lambda \langle \mathcal{D} \rangle}{Q - \lambda \langle \mathcal{D} \rangle + \lambda l}, & \text{when } \langle \mathcal{D} \rangle - \frac{Q}{\lambda} \leq x < l, \\ 1 - \frac{\lambda}{Q} \left\{ \int_x^\infty [1 - G(\eta)] d\eta \right\}, & \text{when } l \leq x. \end{cases} \quad (66)$$

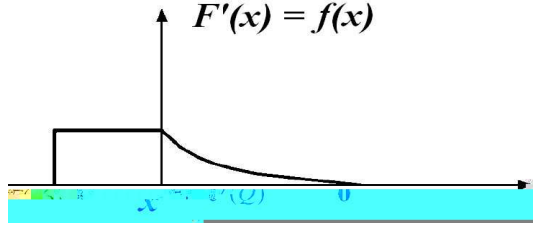


Figure 6: Density of the lead time profile $f(x) = dF(x)/dx$ when $F(Q) < 0$.

Remark. The alternative regimes given by (65) and (66) can be heuristically understood by invoking the *Little law* which connects the average queue length $\langle Q \rangle$ with the average waiting time $\langle W \rangle$, [38],

$$\langle Q \rangle = \lambda \langle W \rangle, \quad (67)$$

a result independent of the scheduling policy. In view of (63) and (67), one obviously suspects that the *LTP* strongly depends on the sign of the difference

$$\langle \mathcal{D} \rangle - \frac{\langle Q \rangle}{\lambda} = \langle \mathcal{D} \rangle - \langle W \rangle.$$

Intuitively, when $\langle W \rangle$ exceeds $\langle \mathcal{D} \rangle$, it is expected, in the average, that processed jobs will be delivered too late and conversely. While the above heuristic arguments is strictly valid only for the averages, [39], were able to show that in heavy traffic regimes, it also holds also for the LTP given in (65) and (66).

Assuming that the arriving tasks have positive deadlines, the LTP as given by (65) and (66) imply:

a). If the left-hand support of the LTP is negative, then a job entering into service is already late, (case of (66)) see Fig. 6.

b). If the left-hand support of the LTP is positive then a jobs enters into service with a positive lead time, (case of (65)) see Fig. 5. Accordingly, it is likely that the tasks will be completed before the deadline expired.

c). The critical value $Q^* = \langle \mathcal{D} \rangle / \lambda$ for which $\mathcal{F}(Q) = 0$, corresponds to a queue length for which customers are likely to become late. Choosing Q exactly to Q^* , we cannot expect lateness to disappear completely but for $Q < Q^*$ lateness will be strongly reduced a behavior clearly confirmed by simulation experiments [32, 39].

d). For deadline distributions $G(x)$ with fat tails, it follows immediately from (65) and (66) that the LTP does possess a fat tail.

4.2.3. "First come first served" (FCFS) scheduling policies

Choosing the deadline probability density as $g(x) = \delta(x)$, (i.e. zero deadline), the EDF scheduling policy directly coincides with the FCFS rule. For this case we have $Q^* = 0$, and (64) implies

$$\mathcal{F}(Q) = \begin{cases} \hat{\mathcal{F}}(Q) = 0, & \text{when } Q \leq 0, \\ -\frac{Q}{\lambda}, & \text{when } Q > 0. \end{cases} \quad (68)$$

Hence the LTP density is given by (65) is merely the uniform probability density $U[-Q/\lambda, 0]$, ($[-Q/\lambda, 0]$ being its support). This expresses the fact that in the heavy traffic regime $\rho = \lambda/\mu \approx 1$, the waiting time behaves as $Q \times (1/\mu) \approx Q \times (1/\lambda)$ leading to a LPT linearly growing with Q . For general $G(x)$, the LTP associated with a FCFS scheduling rule will be given by the convolution of the deadline distribution $G(x)$ with the uniform distribution $U[-Q/\lambda, 0]$. Indeed, adding the task deadlines with the time spent in the queue, we recover the tasks lead-time. Accordingly, in the heavy traffic regime and for a given queue length Q , one explicitly knows the LTP's for both the EDF and the FCFS scheduling policies thus enabling to explicitly appreciate their respective characteristics. In particular, using (65) and (66), one can conclude that for a given queue length Q , with the FCFS scheduling rule and the associated LTP $F(x)$ being the convolution of $G(x)$ with the $U[-Q/\lambda, 0]$, we obtain

$$F(x) = \begin{cases} 0 & \text{when } x < -Q/\lambda, \\ \frac{\lambda}{Q} \int_{-Q/\lambda}^x [G(\xi + Q/\lambda)] d\xi & \text{when } -Q/\lambda \leq x < 0, \\ \kappa + \frac{\lambda}{Q} \left\{ \int_0^x [G(\xi + Q/\lambda) - G(\xi)] d\xi \right\} & \text{when } x \geq 0, \end{cases} \quad (69)$$

where the constant κ reads as:

$$\kappa = \frac{\lambda}{Q} \int_{-(Q/\lambda)}^0 \left[G\left(\xi + \frac{Q}{\lambda}\right) \right] d\xi.$$

The latter equation allows to emphasize the following features:

i). When the left-hand support of the deadline distribution $G(x)$ is larger than Q/λ , the left boundary of the support of $F(x)$ is larger than 0 and therefore the jobs experience no delay when entering into service.

ii). If the left-hand support of $G(x)$ is smaller than Q/λ , then it may happen that the LTP exhibits a negative left-hand support under the FCFS policy and a positive left-hand support under the EDF scheduling rule. Hence in this last situation, the FCFS policy would deliver tasks with lateness while the EDF tasks will be processed in due time. This explicitly confirms intuition that EDF is indeed an efficient policy. It has been shown that the EDF scheduling rule is optimal for minimizing the number of jobs processed after the deadline [46].

iii). If $G(x)$ exhibits a fat tail for $x \rightarrow \infty$ so has the LTP and this whatever the scheduling rule in use. This can be directly verified from (69) by studying the LTP density $f(x) = dF(x)/dx$ for $x \rightarrow \infty$, we have:

$$f(x) = \frac{\lambda}{Q} \left[G\left(x + \frac{Q}{\lambda}\right) - G(x) \right], \quad \text{for } x \rightarrow \infty,$$

which when $G(x) \sim 1 - x^{-q}$ and for $Q/\lambda < \text{const}$ takes the form

$$f(x) \sim x^{-(q+1)}, \quad \text{for } x \rightarrow \infty. \quad (70)$$

Hence, the LTP inherits the fat tail property of $G(x)$ and this even when using the optimal EDF scheduling rule.

Below, we focus on a fully explicit illustration involving the Pareto probability distribution

$$G(x) = \begin{cases} 0 & \text{when } x < B, \\ 1 - \left(\frac{B}{x}\right)^{(\omega-1)} & \text{when } \frac{x}{B} \geq 1, \quad \omega > 1, \end{cases} \quad (71)$$

which has no moment of order $\omega - 1$ or higher. For $\omega > 2$, we have

$$\langle \mathcal{D} \rangle = \left[\frac{\omega - 1}{\omega - 2} \right] B.$$

Using (64) with $l = B$, which implies

$$Q^* = \frac{\lambda B}{\omega - 2},$$

we obtain

$$\mathcal{F}(Q) = \begin{cases} B \left(\frac{B\lambda}{Q(\omega-2)} \right)^{1/(\omega-2)}, & \text{when } Q \leq \frac{\lambda B}{\omega-2}, \\ \left[\frac{\omega-1}{\omega-2} \right] B - \frac{Q}{\lambda}, & \text{when } Q > \frac{\lambda B}{\omega-2}. \end{cases} \quad (72)$$

Using (65) and (66), we can find that the LTP distribution reads as

$$Q \geq \frac{B\lambda}{\omega-2} \Rightarrow F(x) = \begin{cases} 0, & \text{when } x \leq \mathcal{F}(Q), \\ 1 - \frac{\lambda}{Q} \left(\frac{\omega-1}{\omega-2} B - x \right), & \text{when } \mathcal{F}(Q) \leq x < B, \\ 1 - \frac{B\lambda}{Q(\omega-2)} \left(\frac{B}{x} \right)^{\omega-2}. & \text{when } x \geq B. \end{cases} \quad (73)$$

$$Q < \frac{\lambda B}{\omega-2} \Rightarrow F(x) = \begin{cases} 0, & \text{when } x \leq \mathcal{F}(Q), \\ 1 - \frac{B\lambda}{Q(\omega-2)} \left(\frac{B}{x} \right)^{\omega-2}. & \text{when } x > \mathcal{F}(Q). \end{cases} \quad (74)$$

The latter equations describe a fat tail with the exponent $\omega - 2$. It is worth to mention that (74) implies that for $\omega > 2$ and for

$$\frac{Q}{\lambda} < \frac{B}{\omega-2},$$

the EDF scheduling policy part of the tasks enter into the service before the due date expired. Finally note also, that for $\omega \leq 2$, no moments exists for the deadline distribution and hence the theory [39] cannot be applied directly. We conjecture that for these regimes no scheduling rule will be able to deliver tasks in due time.

The results obtained for the LTP, enable us to investigate the asymptotic properties of the waiting time distribution. Indeed, assume a heavy traffic regime with the EDF scheduling policy. Let us also suppose that for a given queue length, some jobs are served too late (i.e., the left boundary of the LTP is negative). As under the EDF rule, the more urgent jobs are always served first, the waiting times of the last jobs in the queue necessarily exceed their deadlines. Therefore, when the deadline distribution exhibits a fat tail, so will the WTD distribution. Note that while the EDF policy decreases, compared with the FCFS rule, the number of jobs served after their deadline, it cannot get rid of the fat tail of the WTD, which is due to the fat tail of $G(x)$. This result is fundamentally different from the situation that is valid for the frozen in time PI models discussed in [33, 47, 48], where the fat tail behavior does not

depend on $G(x)$ itself. This can be heuristically understood as, in [33, 47, 48], the fat tail is mainly due to the low priority jobs, which, as no aging mechanism occurs, are likely to never be served. Note that in [33, 47, 48], stable queuing models (i.e., those for which the traffic) [33] and fat tails of the WTD disappear under a FCFS scheduling rule. Indeed without priority scheduling, the WTD always follows an exponential asymptotic decaying behavior. In the presence of time-dependent PI, all tasks do finally acquire a high priority and this aging mechanism precludes the formation of a fat tail solely due to the scheduling rule. Accordingly, in the presence of aging PI, the appearance of WTD with fat tails is due to $G(x)$.

4.3. The importance of adopting performance scheduling policies

The results for the LTP derived in the preceding section can be directly measured on the actual QS. Consider the queue content of a single-stage QS. Assume that at a given time, Q is the observed queue content, and at this instant take a snapshot of the lead time associated with each waiting item and construct the associated LTP (i.e., the histogram of the observed lead times). In heavy traffic regimes (i.e., typically $0.95 \leq \rho < 1$ leading to stationary average queue lengths $\rho/(1-\rho)$) and under the EDF scheduling policy, the LTP will approximately be given by (65,66). Actual simulation experiments are reported in [43, 44, 39] and [32], where an excellent agreement between measured data and theory is observed.

From the human activity viewpoint, the explicit expressions of the LTP obtained both for the FIFO and EDS policies show clearly that organizing the work scheduling is extremely important. As an illustration, consider a situation in which the deadline distribution $G(x)$ follows an exponential law:

$$G(x) = 1 - e^{-\alpha x} \Rightarrow \langle \mathcal{D} \rangle = \frac{1}{\alpha}. \quad (75)$$

For this situation, we compare two different organization policies:

1. *EDF scheduling policy.* Introducing (75) into (63), we obtain

$$\mathcal{F}(Q) = \begin{cases} -\frac{1}{\alpha} \log\left(\frac{\alpha Q}{\lambda}\right) & \text{when } Q \leq \frac{\lambda}{\alpha}, \\ \frac{1}{\alpha} - \frac{Q}{\lambda} & \text{when } Q > \frac{\lambda}{\alpha}. \end{cases} \quad (76)$$

When $\mathcal{F}(Q) > 0$ (i.e., the upper line in (76)), it follows from (65) that

$$F(x) = \begin{cases} 0 & \text{when } x < \mathcal{F}(Q), \\ 1 - \frac{\lambda(1-\alpha x)}{\alpha Q} & \text{when } \mathcal{F}(Q) \leq x < 0, \\ 1 - \frac{\lambda}{\alpha Q} e^{-\alpha x} & \text{when } 0 \leq x. \end{cases} \quad (77)$$

2. *FIFO scheduling policy.*

With $G(x)$ given by (75), the result given in (69) reads as

$$F(x) = \begin{cases} 0, & x < -\frac{Q}{\lambda}, \\ 1 + \frac{\lambda x}{Q} - \frac{\lambda}{\alpha Q} \left(1 - e^{-\alpha\left(x + \frac{Q}{\lambda}\right)}\right), & -\frac{Q}{\lambda} \leq x < 0, \\ 1 - \frac{\lambda\left(1 - e^{-\frac{\alpha Q}{\lambda}}\right)}{\alpha Q} e^{-\alpha x}, & x \geq 0. \end{cases} \quad (78)$$

Comparing (77) and (78), we conclude that in a heavy traffic regime, for a given work load Q , the use of EDF enables us to process tasks in due time with a high probability while the naive FIFO policy generates large delays.

Specifically, when $Q < \lambda/\alpha$, the EDF policy guarantees that most jobs enter into service before the deadline (see (77)) and will therefore be served before deadline, with a high probability. On the contrary, the FIFO policy result given in (78) (i.e., obtained for $x = 0$ in the last line of (78) shows that a proportion of $1 - (\lambda [1 - e^{-\alpha Q/\lambda}] / \alpha Q)$ jobs enter the service with delays and will therefore be late.

As far as human resources are concerned, this simple model enables us to quantify the importance of adopting performance scheduling policies to respond to the burn out – generating challenge: *deliver more in less time with fewer resources*. Along the same lines, one of the key rules to avoid burnout is to *learn to say no* to new incoming tasks if the queue length exceeds a threshold. In our modeling framework, the critical threshold does depend closely on the level Q^* , above which lately served tasks (and hence complaints) are unavoidable.

5. Power law distributions in Self-Organized Criticality

In the last two decades, a meticulous attention has been drawn to the phenomenon of *self-organized criticality* (SOC), a property of dynamical systems which have a critical point as an attractor, [27, 50, 49, 51]. A notable feature of these models submitted to a power law statistics is that they have no characteristic scales, similarly to the scale invariant systems being in a critical state. However, unlike systems tackled by the critical phenomena theory the critical state in the SOC models seems to be an attractor of the dynamics and seems to be achieved without any tuning of control parameters. It is observed in slowly-driven non-equilibrium systems with extended degrees of freedom and a high level of nonlinearity. The general idea behind SOC models is very appealing. Consider for instance *Zhangs sandpile model* on \mathbb{Z}^2 , where each site has an energy variable which evolves in discrete time-steps according to a simple "toppling" rule: If a variable exceeds a threshold value, the excess is distributed equally among the neighbors. The neighboring sites may thus turn supercritical and the process continues until the excess is "thrown overboard" at the system boundary.

What makes this dynamical rule intriguing is that if the toppling is initiated from a highly excited state, then the terminal state (i.e., the state where the toppling stops) is not the most stable state, but one of many least-stable, stable states. Moreover, the latter state is critical in the sense that further insertion of a small excess typically leads to further large-scale events. Using the sandpile analogy, such events are referred to as avalanches.

From the very beginning, large theoretical efforts have been made in order to understand a true relation between criticality and self-organized criticality both exhibiting a power law behavior [52, 53]. In particular, the use of various *renormalization group techniques* (RG) which proved their exceptional efficiency

in justifying scaling properties in the critical phenomena theory [54] has been in the focus of many studies devoted to the SOC phenomena, [55, 56, 57, 58, 59, 60, 61]. This still deserves a thorough investigation as a potential candidate for the "SOC phenomena theory".

In the critical phenomena theory, the RG method usually helps to establish the long time and large scale asymptotic behavior in infinite systems defined by the stochastic differential equations with the Gaussian distributed external random force [62] that models random boundary conditions. RG is an effective method of studying self-similar scaling behavior in such systems. On the contrary, the majority of models exhibiting SOC phenomena are defined on a finite piece \mathcal{L} of a discrete lattice \mathbb{Z}^d by discrete time dynamical rules [27, 49]. Moreover, in SOC models the energy is usually dissipated at the open boundaries of the lattice piece, while, in the majority of critical phenomena, a quenched distribution of absorbing defects through the lattice is imposed.

The primal goal for the SOC phenomena theory is to investigate the scaling properties of SOC models, in particular, to justify the numerically observed results [63, 64] on the power law distribution of avalanche sizes in sandpile models introduced by Bak, Tang and Wiesenfeld, [27]. In more general formulation, the finite size scaling (FSS) hypothesis [65, 66] is usually assumed in SOC systems,

$$P(x, L) = x^{-\tau_x} \mathcal{F}\left(\frac{x}{L^{\sigma_x}}\right), \quad x \equiv \{s, t, a\}, \quad (79)$$

where $P(x, L)$ is the probability distribution of occurrence of an avalanche of a given size s (the number of sites involved in a relaxation process), area a , and time t , L is the size of the lattice piece. If the FSS Ansatz (79) is valid, then the dynamical exponents τ_x and σ_x determine the universality class of the model [27]-[51]. Within the framework of numerous models, the dynamical exponents τ_x and σ_x are found from the different phenomenological approaches, which are loosely related to underlying microscopic models, and therefore some doubt remains about the universality of representations such as (79), [67, 68, 69].

To identify the scale invariant dynamics, the real-space RG method had been applied to the cellular automaton defined on a 2-dimensional lattice [55, 56]. This approach (*Dynamically Driven Renormalization Group* (DDRG)) deals with the critical properties of the system by introducing in the renormalization equations a dynamical steady state condition which assumes non-equilibrium stationary statistical weights to be used in the calculation [58]. The fixed points of scaling transformations define the dynamical exponents whose value are in a good agreement with computer simulation data. Nevertheless, it has been shown [55] that the fixed points related to these dynamical exponents prescribed by the renormalization group are not accessible from the physical domain of parameter values.

An alternative approach referring to the standard critical phenomena theory is based on the coarse-graining of microscopic evolution rules for the SOC models. In [70, 71] a continuous stochastic partial differential equation related to the randomly driven models had been proposed although the threshold nature of the SOC phenomena was not taken into account. A stochastic partial

differential equation subjected to a threshold condition and driven by a Gaussian distributed external random force acting continuously in time has been discussed in [57, 72, 73].

Therein the external random force introduced into the dynamical equation simultaneously models: first, the noise risen due to elimination of microscopic degrees of freedom; second, unknown (or undefined) boundary conditions; third, a mechanism injecting energy into the system which is supposed to act continuously in time, breaking the time scale separation, and could provoke avalanches to overlap. The threshold condition is taken into account by the Heaviside step function $\theta(x)$. This step function had been regularized as a limit of continuous infinitely differentiable functions and then expanded into power series giving rise to an infinite series of nonlinearities in the stochastic differential equation [57].

Solutions of this nonlinear partial differential equation could be found by iterating in the nonlinearities followed by averaging over the distribution of the random force. Then, the long time large scale asymptotic behavior of the solutions could be established by means of a dynamic RG procedure in the spirit of the dynamic RG-approach [62]. Particularly, the values of dynamical exponents could be found in the form of power series in $\varepsilon = 4 - d$. However, due to an infinite number of nonlinearities risen in the stochastic differential equation by the power expansion of step function, the resulting theory calls for an infinite number of charges (coupling constants) and, therefore, cannot be analyzed in the framework of the standard dynamic RG scheme. In [57], only the first two nonlinear terms have been kept for the RG analysis of the appropriate stochastic problem. All higher order terms had been neglected without any estimation of their contributions to the long time large scale asymptotic behavior. Let us note that the standard power counting analysis of such a model shows convincingly that all these terms are of equal importance for the asymptotic behavior and all of them have to be taken into consideration on equal footing.

It is important to emphasize that the correspondence between the models of deterministic dynamics and the above stochastic problem is indeed questionable and usually lays beyond the studies. The obvious advantage of such a coarse graining approach is that it allows to use the modern critical phenomena techniques of analysis achieving impressive results on the self-similar scaling behavior.

Here, we present the results [59, 61] on the long time large scale asymptotic behavior for the model based on the nonlinear stochastic dynamics equation derived from the coarse-graining procedure from the discrete rules of deterministic dynamics holding all nonlinear terms in check. This task is highly nontrivial and of sufficient interest itself stimulating further developments in modern critical phenomena theory [54].

5.1. Coarse-graining of microscopic evolution rules for SOC-models

Recently, two randomly driven SOC models proposed by Zhang [49] and by Bak *et al.* [27] (BTW) have been connected to stochastic differential equations [57]. For the convenience of the reader, we briefly describe the microscopic rules

of these SOC models. Both models are defined on a finite piece of d -dimensional lattice $\mathcal{L} \subset \mathbb{Z}^d$ in which any site $i \in \mathcal{L}$ can store some continuously distributed variable E_i usually called energy [81].

For Zhang's model, the system is perturbed by a random amount of energy $\delta E > 0$ at a randomly chosen site $i \in \mathcal{L}$. Once the value E_i exceeds a given threshold value E_c , this site becomes active, and transfers all energy to the nearest neighbors. As a result, the neighboring sites can be also activated and transfer energy to the next neighbors, etc. until it is absorbed at the open boundary $\partial\mathcal{L}$. The avalanche ends when all sites reached a value of energy smaller than E_c . The next energy input into the system occurs only when the avalanche has stopped.

For the BTW model, the amount of energy perturbing the system is fixed $\delta E = E_c/q$ where q is a coordination number, and the amount of energy transferred to neighbors from an active site is also fixed at E_c .

For both models, energy is pumped into the system at the small-scale of lattice spacing a and then is transferred to a large scale comparable to the size of \mathcal{L} and actively dissipated at the open boundaries.

For each $i \in \mathcal{L}$, the microscopic evolution rules can be written in the form of a *stochastic coupled map lattice* (SCML),

$$\begin{aligned} E_i(t+1) - E_i(t) & \quad (80) \\ &= \frac{1}{q} \sum_{mm} [(\chi E_{mm}(t) + E_c)\theta(E_{mm}(t)) - (\chi E_i(t) + E_c)\theta(E_i(t))] + \zeta_i(E, t), \end{aligned}$$

in which $E_i(t)$ is the exceed of energy over the critical value E_c , $\chi = 1$ for Zhang's model and $\chi = 0$ for BTW. The external noise

$$\zeta_i(E, t) = (\delta E) \cdot \delta_{i, \mathbf{n}(t)} \prod_{j \in \mathcal{L}} [1 - \theta(E_j(t))] \quad (81)$$

acts at a slow time scale, and is present when there are no active sites in the lattice. Here $\mathbf{n}(t)$ is a random vector pointing the site of the lattice piece \mathcal{L} that is perturbed with energy $(\delta E) > 0$.

The dynamics of avalanches governed by the SCML (80) evolves infinitely fast in comparison with the dynamics of energy feeding. It has been pointed out [57] that the SCML (80) is invariant under spatial translations, rotations, and reflections. Furthermore, if $\chi = 0$, the equation is invariant under a parity transformation of the order parameter, $E \rightarrow -E$. The SCML (80-81) is supplied with the absorbing boundary condition $E_{\partial\mathcal{L}}(t) = 0$.

The SCML (80) can be coarse-grained in order to obtain a continuum stochastic differential equation [57] for the effective continuum scalar field $E(\mathbf{r}, t)$,

$$\frac{\partial E(\mathbf{r}, t)}{\partial t} = \alpha_0 \Delta [(\chi E(\mathbf{r}, t) + E_c)\theta(E(\mathbf{r}, t))] + f(\mathbf{r}, t) \quad (82)$$

where $\alpha_0 > 0$ is the only dimensional parameter in the model, $[\alpha] = L^2 T^{-1}$, and depends on the lattice spacing a , the unit time step, and the coordination

number q . Δ is the Laplace operator. The noise $f(\mathbf{r}, t)$ is a sum of the multiplicative external noise depending on the whole lattice state and the internal noise that appears due to the elimination of microscopic degrees of freedom. In the continuous model, energy is thought to disappear in those regions of lattice where $f(\mathbf{r}, t) < 0$ and to arrive at the points for which $f(\mathbf{r}, t) > 0$. In a stationary state, these processes are obviously balanced, therefore, $\langle f(\mathbf{r}, t) \rangle = 0$.

In [57], the important effect of dissipation at the open boundaries has not been taken into account and a quenched distribution of energy absorbing defects has been assumed. Time scale separation of dynamics has been also neglected, and the noise $f(x)$, $x \equiv \mathbf{r}, t$, has been understood just as a quenched Gaussian process uncorrelated in space and time with a covariance

$$\langle f(x)f(x') \rangle = 2\Gamma\delta^d(\mathbf{r} - \mathbf{r}')\delta(t - t'), \quad (83)$$

which is typical for random walks. In the present section, we use a different Ansatz for the covariance $\langle f(x)f(x') \rangle$ which takes the slow-time scale dynamics of the stochastic force $f(x)$ into account (see the next section).

The continuum stochastic partial differential equation (82) requires a regularization of the step function at zero. Following [57], we use

$$\theta(E) = \lim_{\Omega \rightarrow \infty} \frac{1 + \operatorname{erf}(\Omega E)}{2}, \quad (84)$$

as a regularizing function where $\operatorname{erf}(x) = \pi^{-1/2} \int_{-\infty}^x \exp[-y^2] dy$ is the error function and Ω is the regularization parameter. The reason for this choice of regularization procedure is that it allows a power expansion with an infinite radius of convergence.

Developing (84) in powers of E and substituting the series expansion into (82), one obtains the strongly nonlinear stochastic partial differential equation

$$\frac{\partial E(\mathbf{r}, t)}{\partial t} = \alpha_0 \sum_{n \geq 1} \frac{\lambda_{n0}}{n!} \Delta E^n(\mathbf{r}, t) + f(\mathbf{r}, t), \quad (85)$$

where the effective coupling constants take different values depending on the model:

$$\lambda_{n0} = \lim_{\epsilon \rightarrow \infty} \epsilon^n \left[E_c \theta^{(n)}(0) + \frac{n\chi}{\epsilon} \theta^{(n-1)}(0) \right], \quad n \in \mathbb{N} \quad (86)$$

in which $\theta^{(n)}(0)$ is the n -th order derivative of the regularizing function (84) at zero. The coefficient λ_{n0} becomes formally infinite as $\epsilon \rightarrow \infty$, however, the series in (85) converges. In the equation (85), we have supplied the parameter α_0 and the coupling constants λ_{n0} with index "0" to distinguish their bare values from the renormalized analogs which we shall denote in forthcoming sections simply as α and λ_n consequently. It has been noted [57] that since $\theta^{(2n+2)}(0) = 0$, all even coupling constants vanish for the BTW model, whereas they do not for the Zhang's one. The set of coupling constants λ_{n0} for both models are identical in the limit $\epsilon \rightarrow \infty$.

The equation (85) describes the diffusion of energy in \mathbb{Z}^d issued from a source defined by $f(x)$, $x \equiv \mathbf{r}, t$. This equation (up to a minor change of notations) has been considered in the work [57] in the whole space and the important effect of dissipation at the open boundaries has not been taken into account. Alternatively, a small probability of dissipating an amount of energy E_c/q has been assigned for each site when it topples, instead of transferring it to a certain neighbor. This procedure expresses the *assumption of random boundaries* and corresponds to a model defined on an infinite lattice with a dissipation for each toppling site. We discuss the possible changes to the critical behavior due to the presence of regular absorbing boundary in the section 11.

We study the long time large scale asymptotic behavior in the system governed by the stochastic differential equation (85) in the whole space supposing that the random force $f(x)$ is Gaussian distributed and characterized by the covariance (see the next section) which goes beyond the "white noise" approximation studied in [57]. The introduction of the random force $f(x)$ in (85) expresses the boundary conditions at the *random boundaries* [57].

5.2. Covariance of random forces

The introduction of the random force into the equation (85) phenomenologically models a consequence of the elimination of microscopic degrees of freedom and, at the same time, the injection of energy into the system. We take the time scale separation into account supposing that the dynamics of the slow-time scale and fast-time scale components of the random force are essentially different. Namely, we suppose that in the slow-time scale (i.e., the time scale of energy injection) this dynamics can be taken as the white noise like in [57], $\langle F(x) \rangle = 0$, with the covariance

$$D_F \equiv \langle F(x)F(x') \rangle = 2\Gamma\delta^d(\mathbf{r} - \mathbf{r}')\delta(t - t'), \quad (87)$$

where Γ is the Onsager coefficient. However, in the equation (85) defining the dynamics of relaxation processes evolving in the fast-time scale [57], the random force $f(x)$ introduced into r.h.s. has to be also of fast-time scale. We take it as the generalized random walks governed by the linear Langevin equation

$$\frac{\partial f(x)}{\partial t} + \mathfrak{R}f(x) = F(x), \quad x \equiv \mathbf{r}, t, \quad (88)$$

driven by the slow-time scale "white noise" $F(x)$, where the kernel of the pseudo-differential operator \mathfrak{R} has the form

$$\mathfrak{R}(k) = \rho_0\alpha_0k^{2-2\eta} \quad (89)$$

in the Fourier space. Here, the coupling constant $\rho_0 > 0$ and the exponent $2\eta > 0$ are related to the reciprocal correlation time at wave number k , $t_c(k) = k^{2\eta-2}/\rho_0\alpha_0$. Dimensional considerations show that the coupling constant ρ_0 is related to the characteristic *ultra-violet* (UV) ultra-violet momentum scale in SOC momentum scale $\Lambda \simeq 1/a$ by $\rho_0 \simeq \Lambda^{2\eta}$ and corresponds to microscopic

degrees of freedom expelled from the main equation (85) as a result of the coarse-graining of deterministic dynamical rules [57].

The exponent η corresponds clearly to the anomalous diffusion coefficient [51, 82] $z = 2(1 - \eta)$. Let us note that the scaling form of reciprocal correlation time $t_c(k)$ has interesting connections with the spectrum of Lyapunov exponent, for the Zhang model. It has been indeed shown [82] that the Lyapunov exponents and the corresponding modes relate to the energy transport in the lattice. However, the transport in SOC model is anomalous and the transport modes correspond to diffusion modes in a non-flat metric given by the probability that a site is active. It is remarkable that the Lyapunov spectrum obeys a simple finite scaling form, with an universal exponent $\tau < 1$, which is directly related to η by the relation

$$\eta = \frac{d}{2(1 - \tau)}.$$

The parameter ρ_0 corresponds to the energy injection rate.

It is believed in the literature that the SOC regime corresponds to the case when the injection rate goes to zero, the dissipation rate goes to zero, such that the ratio injection/dissipation goes to zero establishing the time scale separation [55, 56].

In the framework of critical phenomena theory approach to the problems of stochastic dynamics (see [77, 83], for example), the model for the random force covariance D_F in (87) is chosen under the following reasons:

i) for the use of the standard quantum-field RG technique, it is important that the function D_F have a power-law asymptote at large k ;

ii) since the covariance in (87) is static ($\propto \delta(t - t')$), the required *physical* dimension [$\langle FF \rangle$] = $L^d T^{-3}$ is put on by a suitable combination of the only dimensional parameters in the logarithmic theory (α_0 and k);

iii) the "white noise" assumption (87) means that $D_F \propto \text{Const}$ in the Fourier space. To meet this requirement, one introduces a regularization parameter $\varepsilon > 0$ quantifying the deviation from the logarithmic behavior that is similar to the well-know $\varepsilon = 4 - d$ expansion parameter in the critical phenomena theory [54].

All above requirements are satisfied by the model

$$\langle F(\mathbf{k}, \omega) F(-\mathbf{k}, \omega') \rangle \equiv D_F(k) \propto \alpha_0^3 k^{6-d-2\varepsilon}. \quad (90)$$

In this model, 2ε is completely unrelated to the space dimension d (in contrast to the standard critical phenomena approach [54, 77], where usually $\varepsilon = 4 - d$). The logarithmic theory corresponds to the value $\varepsilon = 0$.

Finally, the model for the covariance $D_F(k)$ has to be consistent with the form of the linear operator (89). Namely, from the equation (88), it follows that the covariance $D_f(\omega, k)$ for the pseudo-random force f introduced in the r.h.s. of the main equation (85),

$$\langle f(x) f(x') \rangle = \int \frac{d\omega}{2\pi} \int \frac{d\mathbf{k}}{(2\pi)^d} D_f(\omega, k) \exp[-i\omega(t - t') + i\mathbf{k}(\mathbf{r} - \mathbf{r}')], \quad k \equiv |\mathbf{k}|, \quad (91)$$

is related to $D_F(k)$ as

$$D_f(\omega, k) = \frac{D_F(k)}{\omega^2 + [\rho_0 \alpha_0 k^{2-2\eta}]^2}. \quad (92)$$

Then, it is natural that the spectral density of energy injection,

$$\widetilde{W}(k) = \frac{1}{2} \int \frac{d\omega}{2\pi} D_f(\omega, k), \quad (93)$$

is independent of the correlation time at given wave number, $t_c(k)$. This is true if one takes $D_F(k) \propto \rho_0 k^{-2\eta}$. Eventually, collecting the latter result with the previous Ansatz (90), one arrives at the model

$$D_F(k) = \rho_0 \alpha_0^3 k^{6-d-2\varepsilon-2\eta}. \quad (94)$$

Both exponents 2η and 2ε in (94) are the parameters of the double expansion in the $\eta - \varepsilon$ plane around the origin $\eta = \varepsilon = 0$, with the additional convention that $\varepsilon = O(\eta)$. The positive amplitude factor $\rho_0 k^{-2\eta}$ is considered as a dimensionless coupling constant (i.e., a formal small parameter of the ordinary perturbation theory). For the case of random force uncorrelated in space, $D_F(k) \propto \text{Const}$, the "real" values of ε and η are taken such that $6 - d = 2(\eta + \varepsilon)$. The similar power-law Ansatz for the correlator of random force has been used to model the energy pump into the inertial range of fully developed turbulence [84, 83].

The model (92) where the function $D_F(k)$ is defined by (94) is then more realistic and more reach in behavior than the simple "white noise" assumption (83) discussed in the literature before (for example in the work [57]) since it takes into account the finite correlation time of energy field set by interactions at a level of microscopic degrees of freedom. It has a formal resemblance with the models of random walks in random environment with long-range correlations. We note that the similar correlator for random force has been discussed for the first time in studies devoted to the anomalous scaling of a passive scalar advected by the synthetic compressible flow [85].

The Ansatz (92) that we use contains the previously discussed [57] model (83) as a special case. Indeed, for the rapid-change limit $\rho_0 \rightarrow \infty$, the covariance (92) has the form

$$D_f(\omega, k) \rightarrow \frac{\alpha_0}{\rho_0} k^{2-d-2\varepsilon+2\eta}, \quad (95)$$

and, for $\varepsilon - \eta = 1 - d/2$, one arrives at the model (83) uncorrelated in space and time with $\Gamma = \alpha_0/2\rho_0$.

In the opposite limit of "frozen" configuration of the stochastic force, $\rho_0 \rightarrow 0$, the covariance is static (i.e., independent of time argument ($t - t'$) in t -representation),

$$D_f(\omega, k) \rightarrow \pi \rho_0 \alpha_0^2 k^{4-d-\varepsilon} \delta(\omega). \quad (96)$$

The latter case obviously corresponds to an external random force acting continuously in time. For $\varepsilon = 4 - d$, this random force is uncorrelated in space ($\propto \delta(\mathbf{r} - \mathbf{r}')$).

5.3. An infinite number of critical regimes in SOC-models

Quantum field theory formulation for SOC models has been introduced and studied in [61] following the general approach developed in [78, 79, 76, 84, 83]. All correlation functions $\langle E(x_1) \dots E(x_k) \rangle$, $x \equiv \mathbf{r}, t$, and response functions

$$\langle \delta^m [E(x_1) \dots E(x_k)] / \delta f(x'_1) \dots \delta f(x'_m) \rangle$$

expressing the system response for an external perturbation were renormalized by subtracting all ultra-violet superficial divergences from Green's functions. An infinite number of renormalization constants has been calculated in the one-loop approximation in [61].

Possible scaling regimes of a renormalizable model are associated with the infra-red (IR) stable fixed points of the corresponding differential RG equation. The coordinates of fixed points $\{\rho_*, \lambda_{n*}\}$ in the infinitely dimensional space of coupling constants λ_n of the stochastic model (85) are the solutions of the equations

$$\beta_\rho(\rho_*, \lambda_{n*}) = \beta_n(\rho_*, \lambda_{n*}) = 0, \quad n = 1, 2, \dots, \infty \quad (97)$$

where $\beta_{\rho, n}$ -functions, the coefficients in the differential RG equation, are some rational functions of the parameters ρ and λ_n . Any solution of (97) is an IR-attractive (IR-stable) fixed point of the RG equation if the corresponding Jacobian matrix

$$J_{ik} = \frac{\partial \beta_i}{\partial \lambda_k}$$

is positively defined (i.e., the real parts of all eigenvalues of the matrix J_{ik} are positive) for small $\eta > 0$, $\varepsilon > \eta$, $0 < \rho < 1$, where $\lambda_0 \equiv \rho$ and β_i denotes the complete set of the β -functions of the RG-equation.

It follows from the explicit expressions for an infinite set of β -functions found in [61] that two coordinates of fixed points, λ_{1*} and λ_{2*} , can be chosen arbitrary, then all other coordinates ρ_* and λ_{k*} , $k > 2$ can be found directly from the equations (97). Therefore, the RG differential equation for SOC models has a two-dimensional surface of fixed points spanned with λ_{1*} and λ_{2*} in the infinite dimensional space of coupling constants $\{\rho, \lambda_n\}$.

The complete IR-stability analysis for this manifold of fixed points is a formidable task. In the limiting case of "white noise" model (83), taking formally

$$\rho_* \rightarrow \infty, \quad \eta = 0,$$

it is possible to demonstrate that

$$J_{ik} \approx -(n-1)\varepsilon\delta_{ik} < 0,$$

where δ_{ik} is the Kronecker symbol, so that there are no IR-stable fixed points in SOC for zero correlation time at all wave numbers. The time scale separation is mandatory for the existence of a critical regime in SOC.

In the opposite limit of "frozen" configuration of the stochastic force, the fixed points of the RG equation have been shown also IR unstable, since

$$J_{ik} = -(n-1)\varepsilon\delta_{ik} < 0.$$

In a general setting, the matrix J_{ik} in such a case has a block triangular form, and therefore its eigenvalues coincide with the diagonal elements which can be calculated for any β_n . The stability domains are defined by the roots of polynomials in ρ_* . For instance, the positivity of the first eigenvalues requires that

$$\frac{\rho_*^3 + 3\rho_*^2 - 2 - 4\rho_*}{(1 + \rho_*)(1 + \rho_*^2)} < 0,$$

and

$$\frac{2\rho_*^2 - 3 - 5\rho_*}{(1 + \rho_*)(1 + \rho_*^2)} < 0$$

that is true for $|\rho| < 1$. As n grows up, polynomials of any large order can appear splitting the stability domain into a number of stable and unstable strips.

It is important to note that in a multi-charge theory, even if the IR-stable fixed points of the RG equation exist, the actual trajectory of the system in the multi-dimensional (phase) space of coupling constants (in our case, an infinitely dimensional space $\{\rho, \lambda_k\}$) starting from the given initial values ρ_0, λ_{k0} may not achieve any of them. The trajectory can leave the stability domain (in the critical phenomena theory, it is usually interpreted as the first order phase transition [54, 77]) breaking the scaling asymptote.

5.4. Fat tails in SOC-models

In the IR-stable critical regimes, the Green functions and the response functions exhibit scaling behavior characterized by the following "critical dimensions":

$$\begin{aligned} \Delta[t] &= -\Delta[\omega] = -2 + \gamma_{\alpha*} = 2\eta - 2, \\ \Delta[E] &= 2\eta - \varepsilon, \\ \Delta[E'] &= d + \varepsilon - 2\eta. \end{aligned} \tag{98}$$

We have pointed out before that for the random force uncorrelated in space ($D_F(k) \propto \text{Const}$), the "real" value ε_r is taken such that

$$3 - d/2 = \eta + \varepsilon_r.$$

In two alternative limiting cases, we have

$$\varepsilon_r = 1 - d/2 + \eta$$

(the "white noise" assumption; the system lacks of IR-attractive fixed points) and $\varepsilon_r = 4 - d$ (the "frozen" configuration of the random force). Substituting these values into (98), we obtain different critical dimensions for the energy field $\Delta[E]$ and the auxiliary field $\Delta[E']$ listed in the Tab. 1. For instance, for the critical dimension of the simplest Green function $\langle EE \rangle(\omega, k)$, we obtain

$$\Delta[\langle EE \rangle] = 2\Delta[E] - d + \Delta[t],$$

and

$$\Delta[\langle EE \rangle_{\text{st}}] = 2\Delta[E] - d,$$

Table 1: Critical dimensions of the fields E and E' depending on the various models for the covariance D_F

ε	$\Delta[E]$	$\Delta[E']$
$3 - \eta - d/2$	$d/2 + 3(\eta - 1)$	$d/2 + 3(1 - \eta)$
$1 - d/2 + \eta$	$d/2 + \eta - 1$	$d/2 + 1 - \eta$
$4 - d$	$2\eta - 4 + d$	$4 - 2\eta$

for its static analog,

$$\langle EE \rangle_{\text{st}}(k) = (2\pi)^{-1} \int d\omega \langle EE \rangle^R(\omega, k).$$

The simplest response function $\langle E'E \rangle$ evaluates the average size of the relaxation process arisen in the system as a reaction for a point-wise perturbation; its Fourier transform is the distribution of avalanche size $P(s)$ observed in numerical experiments. For $\langle E'E \rangle$, in the IR-stable critical regime we obtain

$$\begin{aligned} \Delta[\langle E'E \rangle] &= \Delta[E'] \\ +\Delta[E] - d + \Delta[t] &= -2 + 2\eta. \end{aligned} \quad (99)$$

The squared effective radius

$$R^2 = \int d\mathbf{x} \mathbf{x}^2 \langle E(\mathbf{x}, t) E'(\mathbf{0}, 0) \rangle \quad (100)$$

of the relaxation process at a moment of time $t > 0$ started at $t' = 0$ at the origin $\mathbf{x} = 0$, one can find that it scales as

$$\frac{dR^2}{dt} \propto R^{2\eta}. \quad (101)$$

Indeed, since $\Delta[R] = -1$ (by convention),

$$\Delta\left[\frac{dR^2}{dt}\right] = -2 - \Delta[t],$$

from where we have the result (101). The obtained relation is analogous to the well-known Richardson's phenomenological law for the diffusion of passive admixtures in the ambient turbulent flows [80].

We have studied the long time large scale asymptotic behavior for the strongly nonlinear stochastic problem which relates both to the Zhang and BTW models exhibiting the self-organized critical behavior. The proposed model is interesting as itself since it is connected to the problem of nonlinear diffusion of the chemically active scalar advection in the turbulent flows [86]. The stochastic problem has been considered in the bulk, far from a regular boundary. The energy dissipation at the open boundaries has not been taken into account, instead a quenched distribution of energy absorbing defects has been assumed.

We now make several important comments on the further investigations in the framework of RG approach to the stochastic differential equations related to the SOC models.

The first comment is on the possible changes for the critical behavior close to the regular open boundary exhibiting the absorbing property. The equation (85) can be considered in a half-space $z > 0$ where the open boundary coincides with the $z = 0$ plane. Then the effect of boundary would be due to the semi-infinite geometry of the system: The absence of sites from one-half space ($z < 0$) changes the energy transfer along the surface. Using the critical phenomena analogy [88], one can say that the surface does not become critical simultaneously with the bulk, but tends to decouple from the rest of the system. Furthermore, the pseudo-random force acting at the boundary is to be always negative to ensure the complete dissipation of energy,

$$h_{\perp} \equiv f|_{z=0}(\mathbf{r}, t) < 0. \quad (102)$$

This is equivalent to introducing the new field h_{\perp}^0 on the surface that provokes a perturbation which can spread inside the system. These two effects are in competition: If the coordination number q is large, the toppled amount of energy E_c/q dissipated at the open boundary is much smaller than that one transferred to neighbors. In this case, the perturbation risen due to h_{\perp} close to the boundary cannot propagate into bulk. Otherwise, if energy is rather intensively dissipated at the boundary than transferred to the neighboring sites, a critical slope can appear.

Another comment is on possible steps beyond the Gaussian approximation. Let us note that the study of composite operators of the type $(E')^n(x)$ would manage the corrections for the non-Gaussian distributions of random force. We also remember that composite operators are important for the definition of finite size scaling corrections to the leading RG predicted asymptotes.

Scaling, renormalization and statistical conservation laws in the Kraichnan model of turbulent advection in the context of the renormalization group improved perturbation theory have been investigated in [89].

6. Conclusions

Power laws (heavy-tailed) distributions are found throughout many naturally occurring phenomena in physics, and efforts to observe and validate them are an active area of scientific research. We have considered a number of stochastic dynamical models that might generate power law asymptotic distributions. In particular, we have reviewed the stochastic processes involving multiplicative noise, Degree-Mass-Action principle (generalized preferential attachment principle), the intermittent behavior occurring in more complex physical systems near a bifurcation point, some cases of queuing systems, and the models of Self-organized criticality.

These models might be a ground for many natural complex systems. Heavy-tailed distributions appear in them as the emergent phenomena sensitive for

coupling rules essential for the entire dynamics. Relationships between the rules and the power law statistics are strikingly non-linear, as even a small perturbation may cause a large effect, a proportional effect, or even no effect at all.

7. Acknowledgments

We would like to thank Bruno Cessac, Elena Floriani, Max Hongler, and Ricardo Lima for numerous discussions.

References

- [1] M. Levy, S. Solomon, *Int. J. Mod. Phys. C* **7**(4), 595-601 (1996).
- [2] P. Embrechts, C. Klüppelberg, Th. Mikosch, *Modelling Extremal Events for Insurance and Finance*. Berlin: Springer (1997).
- [3] A.-L. Barabási, R. Albert, *Science* **286**, 509-512 (1999).
- [4] H. Takayasu, A.-H. Sato, M. Takayasu, *Phys. Rev. Lett.* **79**, 966 - 969 (1997).
- [5] R. Albert, A.-L. Barabási, *Rev. Mod. Phys.*, **74** (1) (2002).
- [6] A. Lösch, *The Economics of Location*, Yale University Press, New Haven (1954).
- [7] J. Henderson, *Amer. Econ. Rev.* **LXIV**, 640 (1974).
- [8] E. Floriani, D. Volchenkov, R. Lima, *J. Phys. A: Math. Gen.* **36**, 4771-4783 (2003).
- [9] Y. Pomeau, P. Manneville, *Commun. Math. Phys.* **74**, 1889 (1980).
- [10] C. Grebogi, E. Ott, & J.A. Yorke, *Phys. Rev. Lett.* **50**, 93 (1983).
- [11] N. Platt, E.A. Spiegel, & C. Tresser, *Phys. Rev. Lett.* **70**, 279 (1993).
- [12] A.S. Pikovsky, *Z. Phys. B* **55**, 149 (1984).
- [13] L. Yu, E. Ott, Q. Chen, *Phys. Rev. Lett.* **65**, 2935 (1990).
- [14] S.C. Venkataramani, T.M. Antonsen Jr., E. Ott, J.C. Sommerer, *Phys. Lett. A* **207**, 173 (1995).
- [15] S.C. Venkataramani, T.M. Antonsen Jr., E. Ott, J.C. Sommerer, *Physica D* **96**, 66 (1996).
- [16] P.W. Hammer, N. Platt, S.M. Hammel, J.F. Heagy, B.D. Lee, *Phys. Rev. Lett.* **73**, 1095 (1994).

- [17] G. Zumofen, J. Klafter, *Physica D* **69**, 436 (1993).
- [18] J. Redondo, E. Roldán, G.J. de Valcárcel, *Phys. Lett. A* **210**, 301 (1996).
- [19] J.F. Heagy, N. Platt, S.M. Hammel, *Phys. Rev. E* **49**, 1140 (1994).
- [20] N. Platt, S.M. Hammel, J.F. Heagy, *Phys. Rev. Lett.* **72**, 3498 (1994).
- [21] Z. Qu, F. Xie, G. Hu, *Phys. Rev. E* **53**, R1301 (1996).
- [22] H.L. Yang, Z.Q. Huang, E.J. Ding, *Phys. Rev. E* **54**, 3531 (1996).
- [23] Th. Pierre, H. Klostermann, E. Floriani, R. Lima, *Phys. Rev. E* **62**, 7241 (2000).
- [24] J.D. Meiss, *Phys. Rev. A* **34**, 2375 (1986).
- [25] M.E.J. Newman, K. Sneppen, *Phys. Rev. E* **54**, 6226 (1996).
- [26] K. Sneppen, M.E.J. Newman, *Physica D* **110**, 209 (1997).
- [27] P. Bak, C. Tang, K. Wiesenfeld, *Phys. Rev. Lett.* **59**, 381 (1987).
- [28] X.J. Wang, *Phys. Rev. A* **40**, 6647 (1989).
- [29] A. Erdelyi, W. Magnus, F. Oberhettinger, F.G. Tricomi, *Tables of Integral Transforms*, vol **2**, New York: McGraw-Hill (1954).
- [30] Ph. Flajolet, R. Sedgewick, *Analytic Combinatorics*, Cambridge University Press (2009).
- [31] Ph. Blanchard, B. Cessac, T. Krüger, *J. Stat. Phys.* **98**, 375 (2000).
- [32] R.O. Baldwin, N. J. Davis, J.E. Kobza, S.F. Mikdiff. *Queueing Syst. Th. and Appl.* **35**(1-4), 1-21 (2000).
- [33] A.-L. Barabási. *Nature* **435**, 207 (2005).
- [34] Ph. Blanchard, M.-O. Hongler. *Phys. Lett. A* **323** (1-2), 63-66 (2004).
- [35] Ph. Blanchard, M.-O. Hongler, *Phys. Rev. E* **75**, 026102 (2007).
- [36] O.J. Boxma, S.G. Foss, J.M. Lasgouttes, R. Nùñez Queija. *Queueing Systems* **46**, (2004), 35-73.
- [37] F. Brauer & C. Castillo-Chávez, "Mathematical Models in Population Biology and Epidemiology", in *Appl. Math.* **40**, Springer (2001).
- [38] J. Cohen. *J. Appl. Probab.* **10**, 343-353 (1973).
- [39] B. Doytchinov, J. Lehozcky, S. Shreve. *Ann. Appl. Probab.* **11**, 332-378 (2001).

- [40] F. Dusonchet, M.-O. Hongler, *IEEE Trans Robot and Autom.* **19**(6), 997-990 (2003).
- [41] R. Filliger, M.-O. Hongler, *Europhys. Lett.* **70**(3), 285-291 (2005).
- [42] L. Flatto. *The Annals of Probab.* **7**, (2), 382-409 (1997).
- [43] J. Lehozcky, *Real-time queuing theory*, in *Proc. IEEE Real-time system symposium*, New-York, 186-195 (1996).
- [44] J. Lehozcky, *Perfom. Eval.* **25**, 158-168 (1997).
- [45] A.G. Pakes. *J. Appl. Prob.* **12**, 555-564 (1975).
- [46] S. Panwar, D. Townsley, J.K Wolf, *J. of the ACM* **35**,(4), 832-844 (1988).
- [47] A. Vázquez. *Phys. Rev. Lett.* **95**, 248701 (2005).
- [48] A. Vázquez, J.G. Oliveira, Z. Dezsö, K.-I. Goh, Kondor I. A.-L. Barabási. *Phys. Rev. E* **73**(3), 036127 (2006).
- [49] Y.-C. Zhang, *Phys. Rev. Lett.* **63**, 470 (1989).
- [50] P. Bak, *How nature works*, Springer-Verlag (1996).
- [51] H.J. Jensen, *Self-Organized Criticality : Emergent Complex Behavior in Physical and Biological systems*, Cambridge Lecture Notes in Physics **10**, Cambridge University Press (1998).
- [52] D. Sornette, A. Johansen, I. Dornic, *J. Phys. I France* **5**, 325 (1995).
- [53] F. Bagnoli, P. Palmerini, R. Rechtman, *Phys. Rev. E* **55**, 3970 (1997).
- [54] S.K. Ma, *Modern Theory of Critical Phenomena*, Benjamin Reading (1976).
- [55] L. Pietronero, A. Vespignani, S. Zapperi, *Phys. Rev. Lett.* **72**, 1690 (1994).
- [56] A. Vespignani, S. Zapperi, L. Pietronero, *Phys. Rev. E* **51**, 1711 (1995).
- [57] A. Corral, A. Díaz-Guilera, *Phys. Rev. E* **55** (3), 2434 (1997).
- [58] E.V. Ivashkevich, A.M. Povolotsky, A. Vespignani, S. Zapperi, *Phys. Rev. E* **60**, 1239-1251 (1999).
- [59] D. Volchenkov, B. Cessac, Ph. Blanchard, *Int. J. Mod. Phys. B* **16** (8), 1171 (2002).
- [60] P. Le Doussal, K.J. Wiese, *Phys. Rev. E* **79**, 051106 (2009).
- [61] D. Volchenkov, *Eur. Phys. J. Special Topics* **170** (1), pp.1-142 (2009).
- [62] D. Foster, D.R. Nelson, M.J. Stephen, *Phys. Rev. A* **16**, 732 (1977).

- [63] L.P. Kadanoff, S.R. Nagel, L. Wu, S. Zhu, *Phys. Rev. A* **39**, 6524 (1989).
- [64] P. Grassberger, S.S. Manna, *J. Phys. France* **51**, 1077 (1990).
- [65] J.L. Cardy, *J. Phys. A* **17**, L961 (1984).
- [66] J.L. Cardy (ed.), *Finite-size Scaling*, North-Holland, New York (1988).
- [67] R. Pastor-Satorras, A. Vespignani, *Eur. Phys. J. B* **18**, 197-200 (2000).
- [68] M. De Menech, A.L. Stella, *Physica A* **309** (3-4), 289-296 (2002).
- [69] C. Tebaldi, M. De Menech, A. Stella, *Phys. Rev. Lett.* **83**, 3952 (1999).
- [70] T. Hwa, M. Kadar, *Phys. Rev. Lett.* **62**, 1813 (1989).
- [71] G. Grinstein, D.-H. Lee, S. Sachdev, *Phys. Rev. Lett.* **64**, 1927 (1990).
- [72] A. Díaz-Guilera, *Europhys. Lett.* **26**, 177 (1994).
- [73] C.J. Pérez, A. Corral, A. Diaz-Guilera, K. Christensen, A. Arenas, *Int. J. Mod. Phys. B* **10**(10), 1111-1151 (1996).
- [74] J. Collins, *Renormalization: An Introduction to Renormalization, the Renormalization Group, and the Operator-Product Expansion*, Cambridge University Press, Cambridge, (1992).
- [75] P. C. Martin, E. D. Siggia, and H. A. Rose, *Phys. Rev. A* **8**, 423 (1973).
- [76] C. de Dominicis, L. Peliti, *Phys. Rev. B* **18**, 353 (1978).
- [77] J. Zinn-Justin, *Quantum Field Theory and Critical Phenomena*, Clarendon, Oxford (1990).
- [78] H.W. Wyld, *Ann. Phys.* **14**, 143 (1961).
- [79] P.C. Martin, E.D. Siggia, H.A. Rose, *Phys. Rev. A* **8**, 423 (1973).
- [80] A.S. Monin, A.M. Yaglom, *Statistical Fluid Mechanics* **1,2**, MIT Press, Cambridge, Mass. (1971, 1975).
- [81] L. Pietronero, P. Tartagila, Y.-C. Zhang, *Physica A* **173**, 22 (1991).
- [82] B. Cessac, Ph. Blanchard, T. Krüger, *Phys. Rev. E* **64**, 016133 (2001).
- [83] L.Ts. Adzhemyan, N.V. Antonov, A.N. Vasiliev *Field Theoretic Renormalization Group in Fully Developed Turbulence*, Gordon and Breach (1998).
- [84] C. De Dominicis, P.C. Martin, *Phys. Rev. A* **19**, 419 (1979).
- [85] N.V. Antonov, *Phys. Rev. E* **60**, 6691 (1999).
- [86] N.V. Antonov, *Sov. Phys. JTEP* **112** (11), 1649 (1997).

- [87] N.V. Antonov, A.N. Vasiliev, *Sov. Phys. JETP* **108**, 885 (1995).
- [88] E. Brézin, S. Leibler, *Phys. Rev. B* **27**, 594 (1982).
- [89] A. Kupiainen, P. Muratore-Ginanneschi, *J. Stat. Phys.* **126**, 669-724 (2007).